Brief sensory deprivation triggers plasticity of dopamine-synthesising enzyme expression in genetically labelled olfactory bulb dopaminergic neurons

Darren J Byrne[1], Marcela Lipovsek[1,2], Andres Crespo[1], Matthew S Grubb[1]

[1]Centre for Developmental Neurobiology, Institute of Psychiatry, Psychology and Neuroscience (IoPPN), King's College London, London, SE1 1UL, UK

[2]Present address: Ear Institute, University College London, 332 Gray's Inn Road, London, WC1X 8EE, UK

Correspondence: matthew.grubb@kcl.ac.uk

Abstract

In the glomerular layer of the olfactory bulb, local dopaminergic interneurons play a key role in regulating the flow of sensory information from nose to cortex. These dual dopamine- and GABA-releasing cells are capable of marked experience-dependent changes in the expression of neurotransmitter-synthesising enzymes, including tyrosine hydroxylase (TH). However, such plasticity has most commonly been studied in cell populations identified by their expression of the enzyme being studied, and after long periods of sensory deprivation. Here, instead, we used brief 1- or 3-day manipulations of olfactory experience in juvenile mice, coupled with a conditional genetic approach that labelled neurons contingent upon their expression of the dopamine transporter (DAT-tdTomato). This enabled us to evaluate the potential for rapid changes in neurotransmitter-synthesising enzyme expression in an independently identified neuronal population. Our labelling strategy showed good specificity for olfactory bulb dopaminergic neurons, whilst revealing a minority sub-population of non-dopaminergic DAT-tdTomato cells that expressed the calcium-binding protein calretinin. Crucially, the proportions of these neuronal subtypes were not affected by brief alterations in sensory experience. Short-term olfactory manipulations also produced no significant changes in immunofluorescence or whole-bulb mRNA for the GABA-synthesising enzyme GAD67/*Gad1*. However, in bulbar DAT-tdTomato neurons brief sensory deprivation was accompanied by a transient, small drop in immunofluorescence for the dopamine-synthesising enzyme dopa decarboxylase (DDC), and a sustained decrease for TH. Deprivation also produced a sustained decrease in whole-bulb *Th* mRNA. Careful characterisation of an independently identified, genetically labelled neuronal population therefore enabled us to uncover rapid experience-dependent changes in dopamine-synthesising enzyme expression.

35 **Introduction**

36

37 Dopaminergic neurons in the mammalian olfactory bulb form a neurochemically-distinct population
38 of glomerular layer interneurons (Hökfelt *et al.*, 1975; Kosaka & Kosaka, 2007, 2011). They are dual-
39 transmitter cells, releasing both dopamine and GABA to locally modulate information being sent
40 from nose to cortex (Borisovska *et al.*, 2013; Liu *et al.*, 2013, 2016; Banerjee *et al.*, 2015; Pignatelli &
41 Belluzzi, 2017; Vaaga *et al.*, 2017). Production of these transmitters is undertaken by specialised
42 enzymatic pathways, which include tyrosine hydroxylase (TH) as the rate-limiting step in dopamine
43 synthesis, and DOPA decarboxylase (DDC) as its immediate downstream partner (Halász *et al.*, 1977).
44 Glutamate decarboxylase (GAD)-67, on the other hand, is the GABA-synthesising enzyme that is
45 ubiquitously expressed in this neuronal class (Kiyokage *et al.*, 2010; Kosaka *et al.*, 2019).

46 Expression levels of these neurotransmitter-synthesising enzymes are a well characterised target of
47 activity-dependent plasticity in olfactory bulb dopaminergic neurons. TH, especially, is exquisitely
48 sensitive to changes in sensory input. Since the landmark descriptions of decreased TH enzymatic
49 activity and immunofluorescence in the bulb following damage to the peripheral olfactory system
50 (Nadi *et al.*, 1981; Baker *et al.*, 1983), a wealth of evidence has shown that both *Th* mRNA and TH
51 protein levels in bulbar cells track alterations in olfactory sensory neuron activity (Baker *et al.*, 1984,
52 1993, 1999; Kosaka *et al.*, 1987; Baker, 1990; Stone *et al.*, 1990; Cho *et al.*, 1996; Philpot *et al.*, 1998;
53 Saino-Saito *et al.*, 2004; Bastien-Dionne *et al.*, 2010; Cave *et al.*, 2010; Weiss *et al.*, 2011; Grier *et al.*,
54 2016). Indeed, these TH changes are so reliable and sensitive that they are often used as
55 confirmation that particular olfactory system manipulations have been effective (Wilson & Sullivan,
56 1995; Mandairon *et al.*, 2006; Kass *et al.*, 2013). Olfactory bulb GAD67 has received rather less
57 attention, but nevertheless has also been shown to undergo experience-dependent changes in both
58 mRNA (*Gad1*) and protein levels (Parrish-Aungst *et al.*, 2011; Lau & Murthy, 2012; Banerjee *et al.*,
59 2013; Wang *et al.*, 2017).

60 The vast majority of these activity-dependent enzyme expression changes have been detected
61 following relatively prolonged manipulations of sensory input, usually on the order of weeks.
62 However, there are indications that transmitter-synthesising enzyme expression can change more
63 rapidly. A significant decrease in whole-bulb *Th* mRNA has been observed after only 2 d of unilateral
64 naris occlusion (Cho *et al.*, 1996). *In vitro*, increases in TH immunofluorescence or TH-GFP transgene
65 levels have been observed after just 24 h of sustained depolarisation in dissociated and slice
66 cultures, respectively (Akiba *et al.*, 2007; Chand *et al.*, 2015). We also recently found that a 24 h
67 period of *in vivo* sensory deprivation was associated with a decrease in relative immunofluorescence

68 in olfactory bulb TH-positive neurons, without any accompanying change in their density within the
69 glomerular layer (Galliano et al., 2021).

70 A significant caveat is that, to date, these changes in neurotransmitter-synthesising enzyme
71 expression have all been detected either by employing tissue-level analyses that encompass the full
72 range of bulbar cell types, or by using the measured variable itself (e.g. TH immunofluorescence) to
73 identify individual cells to be studied. Ideally, gaining cell-type-specific information regarding
74 plasticity in enzyme expression would instead use an independent marker of cell identity. This
75 would enable experience-dependent changes to be identified amongst a consistently identified
76 group of neurons, without the potential distortion that can result when a plastic variable determines
77 which cells to measure. Here, we therefore took advantage of a conditional mouse transgenic line,
78 $DAT^{IRES\mathit{cre}}$ (Bäckman *et al.*, 2006), which when crossed with an appropriate reporter line generates
79 selective fluorescent label in cells that express the dopamine transporter (DAT-tdTomato). We
80 quantitatively characterised the selectivity of this line and found that it labels a small subset of
81 calretinin-expressing cells in addition to a majority of olfactory bulb dopaminergic neurons.
82 Crucially, this subtype specificity was unaffected by manipulations used to induce brief olfactory
83 deprivation. We found that such short-term, naturally relevant sensory manipulations do not affect
84 relative levels of GAD67 immunofluorescence in olfactory bulb DAT-tdTomato cells, nor whole-bulb
85 levels of *Gad1* mRNA. In contrast, deprivation is associated with decreased whole-bulb *Th* mRNA
86 levels. It also leads to small transient and larger sustained decreases in relative immunofluorescence
87 for DDC and TH, respectively, within an independently identified population of DAT-tdTomato
88 neurons.

Methods

Animals

A total of 69 mice of either sex were used. Mice were housed under a 12 h light:dark cycle in an environmentally controlled room with access to water and food ad libitum. Day of birth was designated as P0. DAT$^{IRES\,cre}$ mice (B6.SJL-*Slc6a3*$^{tm1.1(cre)Bkmn/J}$, Jax stock 006660; Bäckman *et al.*, 2006) were crossed with Rosa26-floxed stop tdTomato reporter mice (Gt(ROSA)26Sor$^{tm9(CAG\text{-}tdTomato)Hze}$, Jax stock 007909) to generate DAT-tdTomato mice. Wild type C57/Bl6 mice (Charles River, Harlow, UK) were used to back cross each generation of transgenic mice. All experiments were performed at King's College London under the auspices of UK Home Office personal and project licences held by the authors.

Unilateral naris occlusion

Olfactory sensory deprivation was induced by unilateral naris occlusion, using a custom made plug (Cummings *et al.*, 1997). Each plug was constructed by knotting suture (Ethilon Monofilament Polyamide 6; Ethicon, Cincinnati, USA) around a piece of unscented dental floss pulled through the lumen of PTFE tubing with an outer diameter of 0.6 mm and inner diameter of 0.3 mm (VWR International, cat#: S1810 04). Mice were briefly anaesthetised with isoflurane and the plug trimmed, coated in petroleum jelly and inserted into the right naris. Mice were returned to their home cage and left for 1 or 3 days before tissue collection. Presence of the nose plug was confirmed by examining the nasal cavity after olfactory bulb dissection *ex vivo*. Sham controls, used for qPCR experiments only, had a nose plug inserted into the right naris and immediately removed. Anaesthetised controls, used for all other experiments, were handled and anaesthetised briefly with isoflurane but had no plug inserted into either naris.

Transcardial perfusion and histology

P28 and P30 DAT-tdTomato mice were anaesthetised with an intraperitoneal overdose of pentobarbital, then transcardially perfused with 20 mL phosphate buffered saline (PBS) with 20 U/mL heparin, followed by 20 mL of 4 % paraformaldehyde (PFA; TAAB Laboratories, Berkshire, UK) in PIPES buffer (3 % sucrose, 60 mM PIPES, 25 mM HEPES, 5 mM EGTA, and 1 mM $MgCl_2$; unless otherwise stated, all reagents were from Sigma). PFA was prepared in batches, frozen at -20 °C and

120 defrosted shortly before use. On completion of perfusion, the mouse was decapitated, and the brain
121 removed from the skull and post-fixed in 4% PFA overnight. The brain was then washed with PBS
122 (3x5 minutes) and stored in PBS with 0.05% sodium azide for up to 6 months. For sectioning, brains
123 were embedded in 6% agarose and sliced coronally at 50 µm using a vibratome (Leica VT1000s;
124 Wetzlar, Germany). Slices were stored in PBS and 0.05% sodium azide at 4 °C before staining.

125

126 *Immunohistochemistry*

127 Immunohistochemical labelling was always performed on 3 slices from each mouse, at
128 approximately 25%, 50% and 75% of the distance along the anteroposterior axis of the olfactory
129 bulb. Free-floating slices were incubated at room temperature (RT; 18-24 °C) for 2 hours in a
130 blocking and permeabilising solution (10% normal goat serum in PBS containing 0.25% Triton-X and
131 0.02% sodium azide). They were then incubated in primary antibody diluted in the blocking solution
132 at 4 °C for between 18-24 hours (see Table 1 for antibodies used and their working dilution;
133 endogenous tdTomato fluorescence was always enhanced with immunolabel for red fluorescent
134 protein; mouse anti-TH antibody was used for all staining except when TH was co-labelled with DDC
135 in Fig.1B, in which case rabbit anti-TH was used to avoid host species cross reactivity). For
136 immunofluorescence intensity analysis, slices were incubated for approximately 72 hours in primary
137 antibody solution. Slices were then washed with PBS (3x5 minutes) and incubated in the species-
138 appropriate secondary antibody (Alexa Fluor® Life Technologies) diluted 1: 1,000 in the blocking
139 solution at RT for 2 hours. After 3x5 minutes washes in PBS, slices were mounted on glass slides with
140 MOWIOL® (Millipore).

141

142 *Image acquisition and experimental design*

143 All images were acquired with a laser scanning confocal microscope (Zeiss LSM 710 Axio Examiner
144 Z1) using appropriate excitation and emission filters, a pinhole of 1 AU and a 40x oil immersion
145 objective. Laser power, gain and offset were manually set to prevent fluorescence saturation and
146 ensure optimum signal-to-noise.

147 For analyses of relative immunofluorescence intensity, we aimed to minimise and control for
148 between-section experimental variability. To reduce the effect of the homecage environment, each
149 experimental 'set' of four mice belonged to the same litter and was exposed to the same external
150 odour environment until unilateral naris occlusion or control procedure at P27. All mice were
151 returned to the homecage and left for 1 or 3 days. Perfusions and post-fixing were performed using

152 **Table 1:** Details of primary antibodies

153

Antigen	Host Species	Working Dilution	Supplier (product code)
Calbindin	Rabbit	1: 5,000	Swant (CB38a)
Calretinin	Mouse	1: 5,000	Millipore (MAB1568)
	Rabbit	1: 5,000	Swant (7699/3H)
cFos	Mouse	1: 1,000	Santa Cruz (sc166940)
Dopa decarboxylase (DDC)	Mouse	1: 1,000	Santa Cruz (sc-293287)
Glutamate decarboxylase 67 (Gad67)	Mouse	1: 500	Millipore (MAB351R)
Red fluorescent protein (tdTomato)	Rabbit	1: 1,000	Clontech (632496)
	Rat	1: 1,000	Chromotek (5F8)
Tyrosine hydroxylase (TH)	Mouse	1: 1,000	Millipore (MAB318)
	Rabbit	1: 1,000	Millipore (AB152)

154

155

156 the same batch of PFA for each set, and mice within each set were perfused within 30 minutes of
157 each other. Brains from the same set were trimmed to the same size and co-embedded in 6%
158 agarose to ensure all brains would be sliced together. The agarose block was cut with landmarks to
159 ensure each mouse could be reliably identified. Co-embedded slices were processed for
160 immunohistochemistry as described above, with primary antibodies applied for 72 hours. Therefore,
161 all control and occluded sections on each slice were exposed to identical reagents at identical
162 concentrations for identical periods of time. The olfactory bulb sections in a co-embedded slice were
163 then imaged on the same day using identical laser and detection settings that were optimised for
164 that co-embedded slice. Z-stacks were taken from different parts of an olfactory bulb slice, setting
165 the start and end Z positions using the DAT-tdTomato fluorescence. Images were acquired at a
166 resolution of 512 x 512 pixels (0.277 µm /pixel) and a Z step of 1 µm.

167 Images for analysing colocalisation of DAT-tdTomato with other markers were acquired at a
168 resolution of 512 x 512 pixels (0.277 µm /pixel) and a Z step of 1 µm, with multiple Z stacks taken
169 around the entire olfactory bulb section.

170 All immunohistochemistry, imaging and image analysis of tissue from mice that had been
171 manipulated was performed blind to experimental group.

172

173 *Image analysis*

174 All image analysis was performed using ImageJ software (Fiji). Cells were counted manually using the
175 cell counter plugin and only if their soma was entirely inside the image area. Soma size and
176 fluorescence intensity were measured at the neuron's widest area in the Z-stack, identified when the
177 soma was larger than in the slice above and below. For measuring immunofluorescence intensity,
178 neurons were manually identified for analysis solely by the expression of DAT-tdTomato. TH and
179 GAD67 immunolabel were located primarily outside the nucleus, therefore, average
180 immunofluorescence intensity (mean grey value; MGV) was measured in the somatic cytoplasm
181 only, using a hand-drawn region of interest (ROI). For DDC and cFos, MGV was measured across the
182 entire soma, again using a hand-drawn ROI. All tdTomato cells that had the entire cell body within
183 the image area and for which the widest soma area could be confirmed were measured in each
184 stack.

185 For immunofluorescence intensity analysis, background MGV values were taken from unlabelled
186 bulbar regions of each Z-stack and were subtracted from the MGV of each cell in that Z-stack. Any
187 resulting negative values (i.e. where background > cell) were set to zero. Normalised percentage
188 immunofluorescence intensity values were then obtained for each cell, by dividing that cell's
189 background-subtracted MGV value by the combined control average in each slice (over both 1 day
190 and 3 day sections), multiplied by 100.

191

192 *Electrophysiology*

193 For acute slice preparation, mice were deeply anaesthetised with isoflurane and decapitated. The
194 olfactory bulb and frontal cortices were rapidly removed and transferred into ice-cold sucrose slicing
195 medium (containing in mM: 240 sucrose, 5 KCl, 1.25 Na_2HPO_4, 2 $MgSO_4$, 1 $CaCl_2$, 26 $NaHCO_3$ and 10
196 D-glucose, bubbled with 95% O_2 °and 5% CO_2). 300 µm horizontal sections of the olfactory bulb were
197 cut using a Leica vibratome (VT1000S; Wetzlar, Germany) and were transferred to standard artificial
198 CSF (ACSF; containing in mM: 124 NaCl, 5 KCl, 1.25 Na_2HPO_4, 2 $MgSO_4$, 2 $CaCl_2$, 26 $NaHCO_3$ and 20 D-
199 glucose; with 10 µM NBQX, 50 µM APV, 10 µM SR-95531 to block major ionotropic synaptic
200 receptors, continuously bubbled with 95% O_2 and 5% CO_2, pH 7.4, ~310 mOsm). Slices were left to
201 recover at RT for at least 45 minutes before experiments began.

202 For whole-cell recordings, individual slices were secured in a chamber mounted on a Nikon FN1
203 microscope. DAT-tdTomato neurons were visualised with a 40x water immersion objective and
204 tdTomato fluorescence was revealed by under LED illumination (pE-100; CoolLED, Andover, UK) with
205 appropriate excitation and emission filters (ET575/50m, CAIRN Research, Kent, UK). Slices were
206 continuously superfused with ACSF heated to physiologically relevant temperature (34 ± 1 C) using
207 an in-line solution heater (TC-344B; Warner Instruments, Kent, UK). Recordings were carried out
208 using a EPC10/2 amplifier coupled to PatchMaster acquisition software (Heka Elektronik, Reutlingen,
209 Germany). Signals were digitised and sampled at 20 kHz. Recording electrodes were pulled from
210 borosilicate glass [outer diameter (OD), 1.5 mm; inner diameter (ID), 1.17 mm] (GT100T-10; Harvard
211 Apparatus, Cambridge, UK) with a vertical puller (PC-10; Narishige, London, UK) and the tip fire-
212 polished with a microforge (MF-830; Narishige, London, UK). Pipettes with 3-5 MΩ resistance were
213 filled with K-gluconate-based intracellular solution, containing, in mM: 124 K-gluconate, 9 KCl, 10
214 KOH, 4 NaCl, 10 HEPES, 28.5 Sucrose, 4 Na_2ATP, 0.4 Na_3GTP, plus 0.15 % biocytin; pH ~7.3, 280-
215 290 mOsm. To study multiple action potential firing, 500 ms somatic current injections of Δ+5 pA
216 were applied from a holding potential of -60 mV in current-clamp mode with 100 % bridge balance,
217 until the point where the neuron entered depolarisation block.

218 After completion of electrophysiology experiments, the pipette was gradually removed with a small
219 amount of positive pressure applied to try and dislodge the patched neuron from the pipette. Once
220 the pipette was separated from the cell, the acute slice was transferred to 4% PFA. The slice was
221 fixed overnight at 4° C, washed with PBS (3x5 minutes) and stored in PBS and 0.05 % sodium azide at
222 4° C, for up to 3 months. Standard immunohistochemistry protocols were used (see above).
223 Streptavidin 488 (Alexa Fluor® Life Technologies) diluted 1: 1,000 was included with the secondary
224 antibodies to label biocytin in the patched neuron.

225

226 *Quantitative PCR*

227 All experimental steps for qPCR were performed in compliance with the MIQE guidelines (Bustin *et*
228 *al.*, 2009). One or 3 days after naris occlusion or control sham surgery, wild-type mice were
229 sacrificed by cervical dislocation followed by decapitation. The brain was quickly removed and
230 placed in cold PBS. The right olfactory bulb was dissected and placed in RNAlater (Thermo Fisher
231 Scientific) overnight at 4° C and stored at -20° C until further processing. Total RNA extraction was
232 performed using the RNAqueous® Micro Kit (Life Technologies). RNA was eluted in 20 µl of elusion
233 buffer and quantified using Nanodrop (Thermo Fisher Scientific) and Qubit (RNA HS Assay Kit, Life
234 Technologies). 300-500 ng of total RNA were used for cDNA synthesis with SuperScript™ II Reverse

235 Transcriptase (Life Technologies), 0.5 mM dNTPs (Life Technologies), 5 µM OligodT23VN (IDT),
236 10 µM DTT (Life Technologies) and 0.2 Units RNase inhibitor (SUPERase•In™, Invitrogen). RNA was
237 denatured for 5 min at 65° C, before adding the reaction mix. Retrotranscription was performed at
238 42° C for 90 min, followed by 20 min at 70° C for enzyme inactivation. Standard RT-PCRs were run for
239 all samples, including non-template controls, to corroborate amplification of single bands of the
240 appropriate size. Cycling conditions were: 95° C for 3 min, (95 C, 15 s; 65-55° C (-0.5° C per cycle),
241 20 s; 68° C, 25 s), 20 cycles, (95° C, 15 s; 55° C, 20 s; 68° C, 25 s), 20 cycles, 68° C, 5 min, 4° C, hold.
242 Reactions were run on a SimpliAmp™ Thermal Cycler (Applied Biosystems). Primers used were:
243 ActB_For, cctctatgccaacacagtgc; ActB_Rev, cttctgcatcctgtcagcaa; Th_For, tgcctcctcacctatgcact;
244 Th_Rev, gtcagccaacatgggtacg; Gad1_For, caagttctggctgatgtgga; Gad1_Rev, cttggcgtagaggtaatcagc;
245 Tbp_For, agggattcaggaagaccacat; Tbp_Rev, cagtggtaccaaaactgactgg; cFos_For,
246 agggagctgacagatacactcc; cFos_Rev, tgcaacgcagacttctcatc; Ddc_For, cacagaagtcattcttgggttg; Ddc_Rev,
247 gagtttcgttcaactcattgga. Primers were designed using the Universal Probe Library Assay Design Centre
248 (Roche), compatible with UPLs 157 (*ActB*), 3 (*Th*), 1 (*Gad1*), 2 (*Tbp*), 94 (*cFos*) and 38 (*Ddc*) primer
249 pairs.

250 qPCR reactions were run using the FastStart Essential DNA Probes Master mix (Roche) on the
251 LightCycler ® 96 Real-Time PCR System (Roche). Final primer concentration was 0.5 µM and probe
252 concentration was 0.1 µM. Cycling conditions were: 95° C for 10 min, (95° C, 10 s; 60° C, 30 s),
253 55 cycles, 4° C, hold. Technical duplicates were performed for all samples and reactions. ActB was
254 used as housekeeping reference gene for Th and Gad1, and Tbp for Ddc and cFos expression
255 quantification. Amplification efficiency for all primer pairs was determined by obtaining a standard
256 curve. Briefly, the cDNAs from each cDNA synthesis reaction were pooled and serially diluted. qPCR
257 reactions were performed as above. Ct amplification curve values were plotted as a function of
258 dilution factor and the amplification efficiency determined from the slope of the linear regression as
259 in $E = 10^{(-1/slope)}-1$. Amplification efficiency (E ± SE) for ActB primers was 1.07 ± 0.02, for Th primers,
260 1.01 ± 0.03, for Gad1 primers, 0.98 ± 0.04, for Tbp primers, 1.02 ± 0.02, for Ddc primers, 0.97 ± 0.04
261 and for cFos primers, 0.97 ± 0.04. Fold changes in Th, Gad1, cFos and Ddc expression levels were
262 obtained using the $2^{(-ddCt)}$ method (Livak & Schmittgen, 2001; Taylor *et al.*, 2019), first normalising Ct
263 levels for each sample to housekeeping Ct levels and subsequently normalising to the average of the
264 control (sham) conditions.

265

266

267

Statistical analysis

Statistical analysis was carried out using Prism (GraphPad, San Diego, USA), Matlab (Mathworks, Massachusetts, USA) or SPSS (IBM). All datasets were described as mean ± SEM, unless otherwise stated, n values reported in the text refer to number of cells, and N values refer to number of mice. Details of all individual statistical tests are reported alongside the appropriate results. α values were set to 0.05 (except where a Bonferroni correction was carried out for multiple comparisons) and all comparisons were two tailed. For multiple group comparisons with multilevel ANOVA followed by Bonferroni post-tests, all groups either passed the D'Agostino and Pearson omnibus test for normality (GraphPad Prism), and/or could be fitted by a Gaussian distribution that explained ≥ 90 % of their variance (custom Matlab script written by MSG). Fisher's exact test was performed when analysing proportions. Due to the design of this test, data had to be analysed twice, by combining groups based on manipulation and then duration of manipulation. A Bonferroni correction was therefore carried out for multiple comparisons in this instance ($\alpha = 0.05/2 = 0.025$). qPCR normalised expression data were obtained from entirely separate 1 d (occluded versus control) and 3 d (occluded versus control) experiments, performed independently with different sets of reagents and with independent normalisation. For this reason we analysed these data with separate unpaired t-tests (with Welch's correction where necessary where SDs were significantly different) for 1 day and 3 day samples. This therefore also required Bonferroni correction for multiple comparisons: again, $\alpha = 0.05/2 = 0.025$.

287 **Results**

288

289 *Using DAT-tdTomato mice to label olfactory bulb dopaminergic neurons*

290 We used a conditional genetic strategy to label dopaminergic neurons in the olfactory bulb by
291 crossing DAT$^{IRES cre}$ mice (Bäckman *et al.*, 2006) with a floxed tdTomato reporter line. This resulted in
292 strong tdTomato fluorescence in small cells surrounding glomerular neuropil in the glomerular layer,
293 along with the odd scattered tdTomato-positive cell in the superficial external plexiform layer (EPL),
294 in keeping with previous reports of dopaminergic cell localisation within the olfactory bulb (Fig. 1A;
295 (e.g. Hökfelt *et al.*, 1975; Banerjee *et al.*, 2013; Kosaka *et al.*, 2019). To confirm the identity of these
296 DAT-tdTomato neurons, we co-stained fixed olfactory bulb slices from juvenile postnatal day (P)28
297 mice for the rate-limiting enzyme in the synthesis of dopamine, tyrosine hydroxylase (TH). Although
298 necessary for both dopamine and noradrenaline production, the absence of local noradrenergic cells
299 in the olfactory bulb (Hökfelt *et al.*, 1975; Rosser *et al.*, 1986) makes TH a selective marker for
300 dopaminergic neurons in this region. Previous analysis of this transgenic line found that ~90 % of
301 TH-positive glomerular layer neurons were also positive for tdTomato (Galliano et al., 2018);
302 however, the composition of the tdTomato-positive population has not yet been fully described. In
303 control animals we found a high incidence of co-labelled neurons, with ~75% of DAT-tdTomato cells
304 staining positively for TH (Fig. 1B,C; % of tdTomato-positive neurons ± SEM: TH-positive, 74 ± 4 %;
305 TH-negative, 26 ± 4 %; n = 598 cells, N = 3; Vaaga *et al.*, 2017). However, by no means all genetically
306 labelled cells in the DAT-tdTomato mouse were TH-positive. We reasoned that the ~25 % of non-TH-
307 expressing DAT-tdTomato cells might be 'true' dopaminergic neurons that have low, undetectable
308 levels of TH expression due to long-term activity-dependent down-regulation (e.g. Baker *et al.*,
309 1983). However, co-staining for another dopamine-synthesising enzyme dopa decarboxylase (DDC),
310 the expression of which is known to be resistant to long-term changes in ongoing activity (Stone *et*
311 *al.*, 1990; Baker *et al.*, 1993; Cave *et al.*, 2010), showed that this is not the case. We found very good
312 agreement between TH- and DDC-positive cells in the olfactory bulb glomerular layer (Fig. 1B;
313 99 ± 0.5 % of TH-positive neurons were also DDC-positive; 89 ± 2 % of DDC-positive neurons were
314 also TH-positive; n = 598; N = 3), but we found only 3 % of DAT-tdTomato cells were positive for DDC
315 without expressing TH (Fig. 1B,C; % of tdTomato-positive neurons ± SEM: TH- and DDC-positive,
316 74 ± 4 %; DDC-positive but TH-negative, 3 ± 7 %; TH-positive but DDC-negative, 0.5 ± 0.3 %; TH- and
317 DDC-negative, 23 ± 2 %; n = 598; N = 3).

318 If ~20-25 % of DAT-tdTomato cells in the olfactory bulb are therefore non-dopaminergic, what type
319 of cell are they? Red fluorescent neurons never had the large, pear-shaped soma characteristic of

320 local excitatory neurons, the external tufted cells, in the glomerular layer (Hayar *et al.*, 2004). This
321 made them most likely to be GABAergic juxtaglomerular interneurons, which in mouse are divided
322 into three mutually exclusive subgroups expressing either TH or the calcium-binding proteins
323 calbindin and calretinin (Kohwi *et al.*, 2007; Kosaka & Kosaka, 2007; Panzanelli *et al.*, 2007; Parrish-
324 Aungst *et al.*, 2007). We never observed any DAT-tdTomato neurons that co-labelled for calbindin
325 (Fig. 1D), but we did find DAT-tdTomato cells that were positive for calretinin (Fig. 1E; Ninkovic *et al.*,
326 2010). Indeed, the tdT-positive/TH-negative subgroup was almost entirely accounted for by cells
327 expressing calretinin (Fig. 1E, F; % of tdTomato-positive neurons ± SEM: TH-positive only, 74 ± 2 %;
328 calretinin-positive only, 22 ± 0.9 %; n = 1404; N = 3). Importantly, although we observed some rare
329 tdTomato-positive cells that were neither TH- nor calretinin-positive (Fig. 1F; tdTomato-positive
330 only, 4 ± 1%, consistent with the 3 % of tdTomato cells found above to be DDC-positive but TH-
331 negative), we never saw any tdTomato-positive cells co-labelled for both TH and calretinin
332 (n = 0 / 1404 cells from N = 3 mice). This suggests that the calretinin-positive DAT-tdTomato cells are
333 non-dopaminergic calretinin neurons that have at least transiently activated DAT expression at some
334 point in their history, rather than being dopaminergic neurons that also co-express calretinin.

335 To check these cells' distinct properties, we obtained whole-cell patch-clamp recordings of DAT-
336 tdTomato neurons in acute olfactory bulb slices. Although these cells are structurally fragile and
337 extremely difficult to recover for post-recording histology (Galliano *et al.*, 2018), we were able to
338 find very rare example neurons that had been successfully filled with biocytin during our recordings
339 and then co-labelled for glomerular layer markers. While a confirmed TH-positive DAT-tdTomato
340 neuron had characteristic multiple spike production in response to a prolonged 500 ms current
341 injection in current-clamp, the one calretinin-positive tdTomato cell we managed to recover
342 displayed only a single, small spike followed by a sustained depolarised plateau potential, as
343 previously described to be typical of this bulbar cell type (Fig. 1G; Fogli Iseppe *et al.*, 2016; Benito *et*
344 *al.*, 2018). The calretinin-positive cells labelled in DAT-tdTomato mice are therefore likely to share
345 their major features with the general population of calretinin-expressing juxtaglomerular neurons.

346

347 **Figure 1**

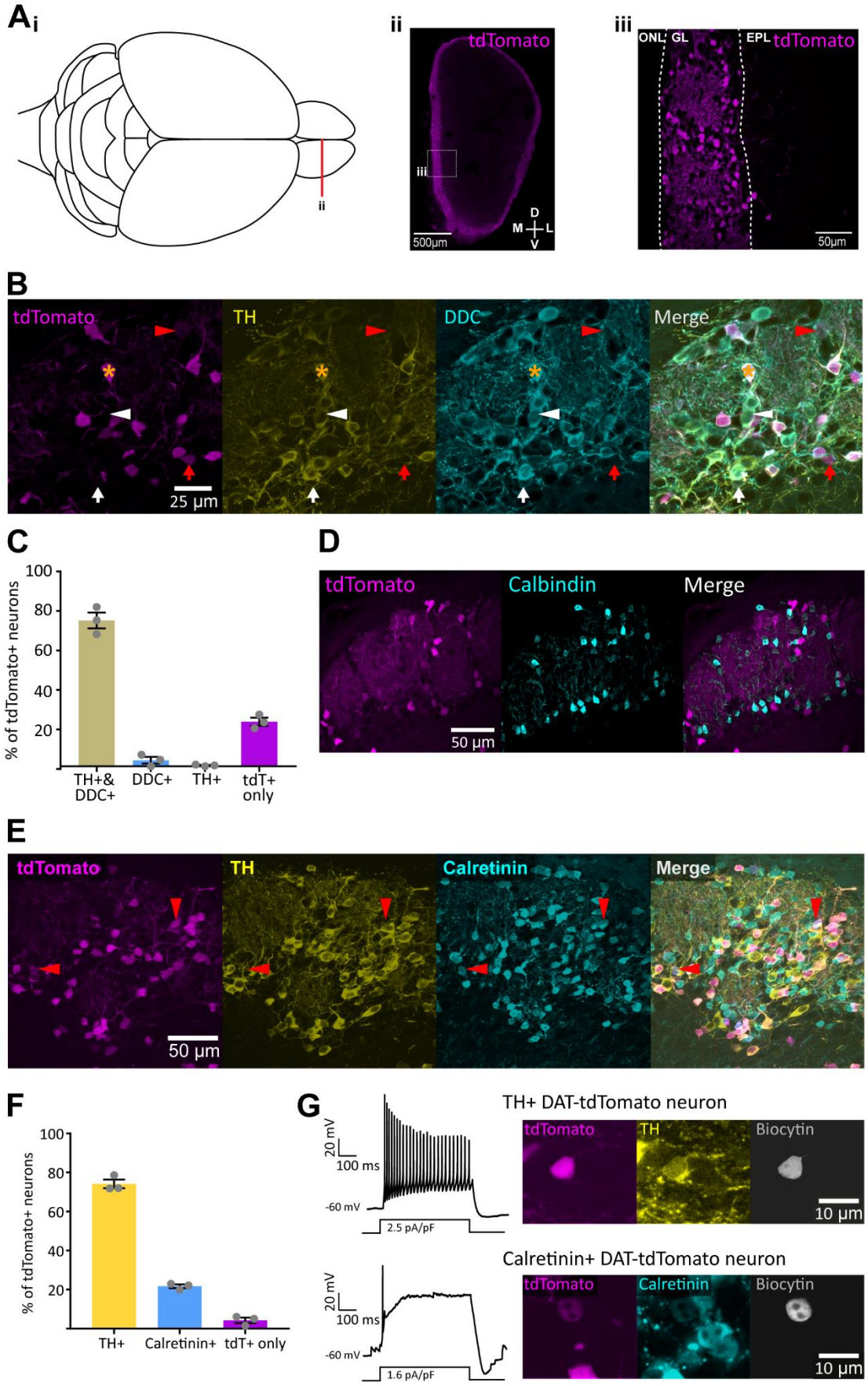

348

349 **Figure 1**. Cell-type identity of olfactory bulb DAT-tdTomato neurons. **A)** tdTomato label in DAT-tdTomato olfactory bulb; **i)**
350 aerial view diagram of mouse brain, showing location of olfactory bulb coronal section in **ii**; **ii)** coronal section of olfactory
351 bulb from a DAT-tdTomato mouse; box shows location of detail in **iii**; **iii)** tdTomato-positive neurons are located
352 predominantly in the olfactory bulb's glomerular layer (GL); ONL, olfactory nerve layer; EPL, external plexiform layer. **B)**
353 Example maximum intensity projection images from the glomerular layer in the olfactory bulb of a control DAT-tdTomato
354 mouse, showing co-label for TH and DDC. Star indicates location of a neuron showing expression of all three markers.
355 Arrowheads indicate location of neurons expressing two markers: red = DAT-tdTomato and DDC; white = TH and DDC.
356 Arrows indicate location of neurons expressing a single marker: red = DAT-tdTomato; white = DDC. **C)** Mean ± SEM
357 percentage of tdTomato+ neurons positive for TH and/or DDC. Grey circles indicate percentages from individual mice. **D)**
358 Example maximum intensity projection images showing immunofluorescence for calbindin in the olfactory bulb glomerular
359 layer of a control DAT-tdTomato mouse. **E)** Example maximum intensity projection images showing immunofluorescence
360 for TH and calretinin in the glomerular layer of the olfactory bulb in a control DAT-tdTomato mouse. Red arrowheads
361 indicate example neurons expressing DAT-tdTomato and calretinin, but not TH. **F)** Mean ± SEM percentage of tdTomato+
362 neurons expressing TH and calretinin. Grey circles indicate percentages from individual mice. **G)** Action potential firing
363 patterns in response to 500 ms somatic current injection (left) and immunohistochemical characterisation (right) in
364 example biocytin-filled DAT-tdTomato neurons that were co-labelled for either TH (top) or calretinin (bottom).

365

366

367 *Sensory deprivation via brief unilateral naris occlusion reduces cFos expression in olfactory bulb DAT-*
368 *tdTomato neurons*

369 Having shown that the DAT-tdTomato mouse line labels olfactory bulb neurons that are
370 predominantly dopaminergic but include a distinct subset of calretinin-positive cells, we went on to
371 use this line for naturally-relevant manipulations of sensory experience (Fokkens *et al.*, 2012;
372 Galliano et al., 2021). In juvenile mice from postnatal day (P)27, we induced brief 1- or 3-day periods
373 of sensory deprivation without damaging the olfactory epithelium, via unilateral naris occlusion with
374 a plastic plug (Fig.2A; Cummings *et al.*, 1997; Kikuta *et al.*, 2015; Cheetham *et al.*, 2016; Galliano et
375 al., 2021). Because of interpretational issues caused by abnormal airflow through the contralateral
376 naris in such manipulations (Coppola, 2012; Kass *et al.*, 2013), we did not compare deprived versus
377 spared olfactory bulbs in the same animals, and instead made all comparisons between the right
378 bulbs of individual occluded or control mice (see Methods).

379 To first validate the effectiveness of our sensory deprivation approach for reducing overall olfactory
380 bulb activity, we assessed levels of whole-bulb mRNA for the immediate early gene *cFos* using qPCR
381 in wild-type mice. We found decreases in *cFos* mRNA after both 1 day or 3 day naris occlusion
382 compared to time-matched sham controls (Fig.2B). The 1 day effect was highly significant, while
383 variability within the 3 day control group meant that the effect of occlusion at this time point fell just
384 short of significance after correction for multiple comparisons (1 day mean ± SEM fold change:
385 sham, 1.11 ± 0.12; occluded, 0.31 ± 0.046; Welch's t-test with $\alpha = 0.025$, $t_{18.25} = 6.45$, $p < 0.0001$,
386 N = 29; 3 day: sham, 1.36 ± 0.38; occluded, 0.42 ± 0.13; Welch's t-test with $\alpha = 0.025$, $t_{8.50} = 2.33$,
387 $p = 0.046$; N = 16).

388 To specifically assess the effect of brief sensory deprivation on spontaneous activity levels in DAT-
389 tdTomato neurons, we then examined cFos immunofluorescence (Liu *et al.*, 1999). Co-embedding
390 olfactory bulbs from all four treatment groups (Fig. 2A; 1 day control, 1 day occluded; 3 day control;
391 3 day occluded) prior to sectioning allowed the best possible consistency in immunostaining
392 protocols (see Methods; Vlug *et al.*, 2005; Galliano et al., 2021). It also enabled us to normalise
393 labelling intensity within co-embedded sets in order to combine analyses across multiple individuals.
394 With this approach we found that DAT-tdTomato cells from occluded mice had significantly lower
395 cFos immunofluorescence after both 1 and 3 days of occlusion (Fig. 2C-E; normalised intensity (%)
396 mean ± SEM: 1 day control, 102.50 ± 3.83%, n = 316 cells, N = 2 mice; 1 day occluded, 56.85 ± 2.10%,
397 n = 358, N = 2; 3 day control, 97.53 ± 3.30%, n = 317, N = 2; 3 day occluded, 62.87 ± 2.63%, n = 309, N
398 = 2. Multi-level ANOVA controlling for set variance, effect of manipulation, $F_{1,1298} = 60.73$, $p < 0.0001$;
399 effect of time, $F_{1,1298} = 1.40$, $p = 0.24$; effect of manipulation x time interaction, $F_{1,1299} = 3.40$, p =

400 0.065. Bonferroni post- test comparing control versus occluded ($\alpha = 0.025$): 1 day, $F_{1,673} = 115.76$, $p <$
401 0.00005; 3 day, $F_{1,626} = 68.56$, $p < 0.00005$). Brief sensory deprivation therefore reliably lowers
402 activity levels in olfactory bulb DAT-tdTomato neurons, and does so in a sustained manner over 1 to
403 3 days.

404

Figure 2

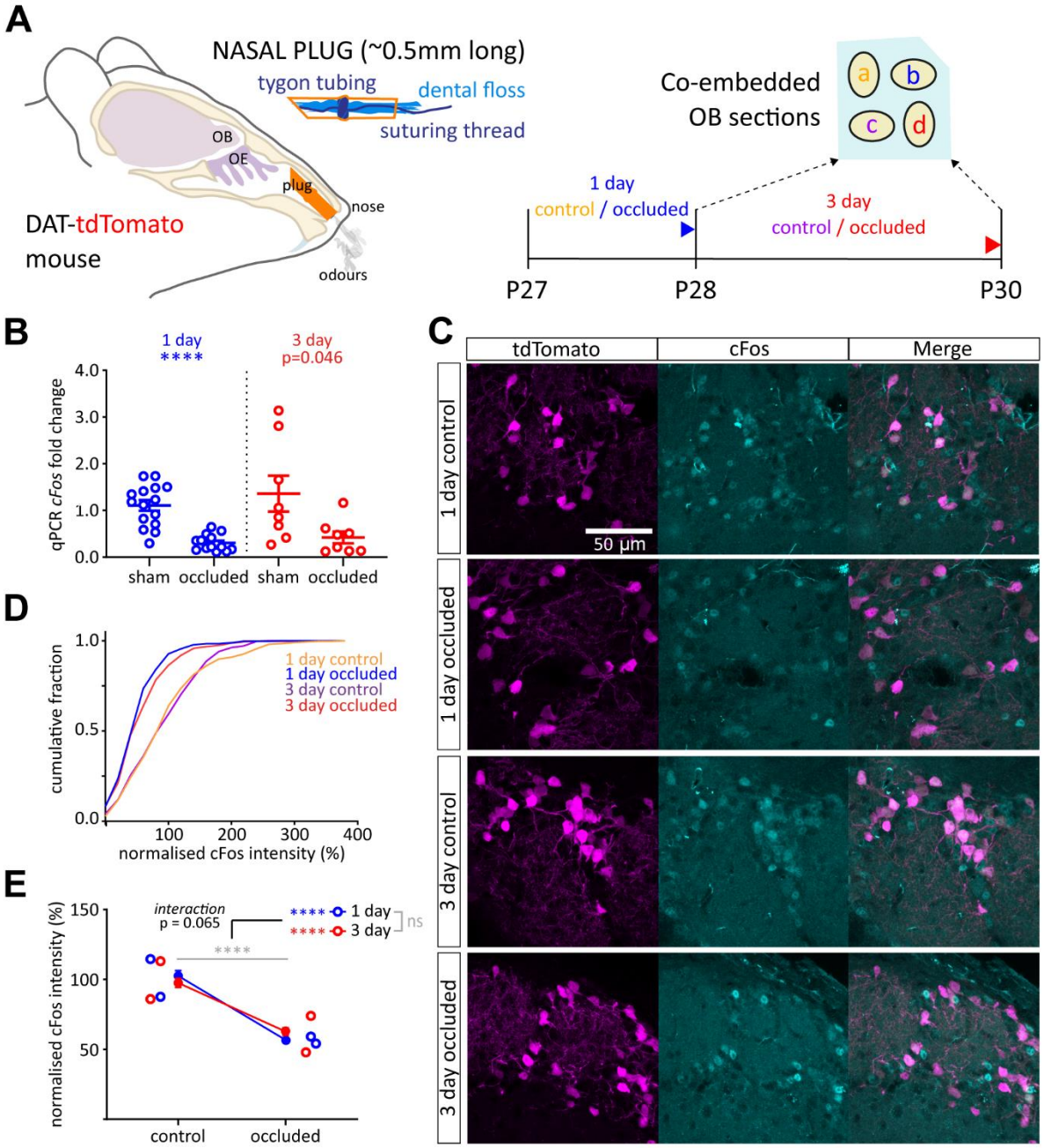

Figure 2. Sensory deprivation via brief unilateral naris occlusion reduces cFos expression in olfactory bulb DAT-tdTomato neurons. **A)** Schematic of naris occlusion protocol and tissue co-embedding for comparison of relative immunofluorescence. OE, Olfactory epithelium; OB, Olfactory bulb; P, Postnatal day; a, 1 day control; b, 1 day occluded; c, 3 day control; d, 3 day occluded. **B)** *cFos* mRNA expression by whole-bulb qPCR. Circles show fold change for individual bulbs vs relevant sham control mean; lines show mean ± SEM fold change for each group. t-test ($\alpha = 0.025$); 1 day, ****, $p < 0.0001$; 3 day, $p = 0.046$. **C)** Example maximum intensity projection images showing immunofluorescent label for cFos in the glomerular layer of the olfactory bulb in 1 and 3 day control and occluded DAT-tdTomato mice. All images are from the same co-embedded preparation, acquired and presented with identical settings. **D)** Cumulative distribution of normalised cFos intensity (%) in DAT-tdTomato neurons in each treatment group. **E)** Line plots showing overall mean ± SEM normalised cFos intensity (%) in each treatment group; unfilled circles show mean normalised cFos intensity (%) for individual mice. Multi-level ANOVA controlling for set variance; effect of manipulation, **** $p < 0.0001$; effect of time, ns: non-significant. Bonferroni post-test ($\alpha = 0.025$); 1 day, effect of manipulation, **** $p < 0.00005$; 3 day, effect of manipulation, **** $p < 0.00005$

420 *Brief naris occlusion does not alter the sub-type composition of olfactory bulb DAT-tdTomato neurons*

421 Given the mixed dopaminergic and calretinin-expressing nature of the population labelled in the
422 DAT-tdTomato mouse olfactory bulb (Fig. 1), it was important to check whether our effective short-
423 term sensory manipulations (Fig. 2) altered this sub-type composition in any way. Crucially, we
424 found no change in the proportion of DAT-tdTomato cells that were calretinin-positive after 1 or 3
425 days of sensory deprivation (Fig. 3A,B; % of calretinin-positive DAT-tdTomato neurons; 1 day control,
426 20.95 %, n = 506, N = 3; 1 day occluded, 24.50 %, n = 502, N = 3; 3 day control, 23.91 %, n = 343, N =
427 2; 3 day occluded, 23.74 %, n = 417, N = 3. Fisher's exact test with $\alpha = 0.025$, effect of manipulation,
428 $p = 0.22$; effect of time, $p = 0.40$).

429 Olfactory bulb dopaminergic neurons are not a unitary, homogeneous cell type (Galliano *et al.*, 2018;
430 Kosaka *et al.*, 2019), so it was also important to assess the representation of dopaminergic subtypes
431 amongst DAT-tdTomato neurons following sensory deprivation. Work from our laboratory and
432 others has identified a key distinction between, on the one hand, small-soma olfactory bulb
433 dopaminergic cells that lack an axon and can be generated throughout life and, on the other, large-
434 soma olfactory bulb dopaminergic cells that possess an axon and are exclusively generated in early
435 embryonic development (Galliano *et al.*, 2018; Kosaka *et al.*, 2019). The latter large-soma sub-
436 population, although present, is significantly under-represented by DAT-tdTomato label, which is
437 dominated by small-soma anaxonic cells (Galliano *et al.*, 2018). Using a previously established soma
438 area cut-off value of 70 μm^2 to define olfactory bulb dopaminergic cells as 'small' (Galliano *et al.*,
439 2018), we confirmed here that this subtype accounts for > 90 % of DAT-tdTomato neurons
440 (Fig.3C,D). Crucially, the high proportion of such small cells represented in the DAT-tdTomato line –
441 which will also include the small-soma calretinin-positive subgroup (Parrish-Aungst *et al.*, 2007) –
442 was not significantly affected by 1 or 3 day naris occlusion (Fig.3D; % of 'small' cells; 1 day control,
443 95.22 %, n = 460, N = 3; 1 day occluded, 91.18 %, n = 408, N = 3; 3 day control, 93.62 %, n = 298, N =
444 2; 3 day occluded, 96.75 %, n = 461, N = 3. Fisher's exact test with $\alpha = 0.025$, effect of manipulation,
445 $p = 0.75$; effect of time, $p = 0.067$). Brief periods of sensory deprivation therefore do not
446 significantly alter the cellular sub-composition of olfactory bulb glomerular layer neurons labelled in
447 DAT-tdTomato mice.

448

449 **Figure 3**

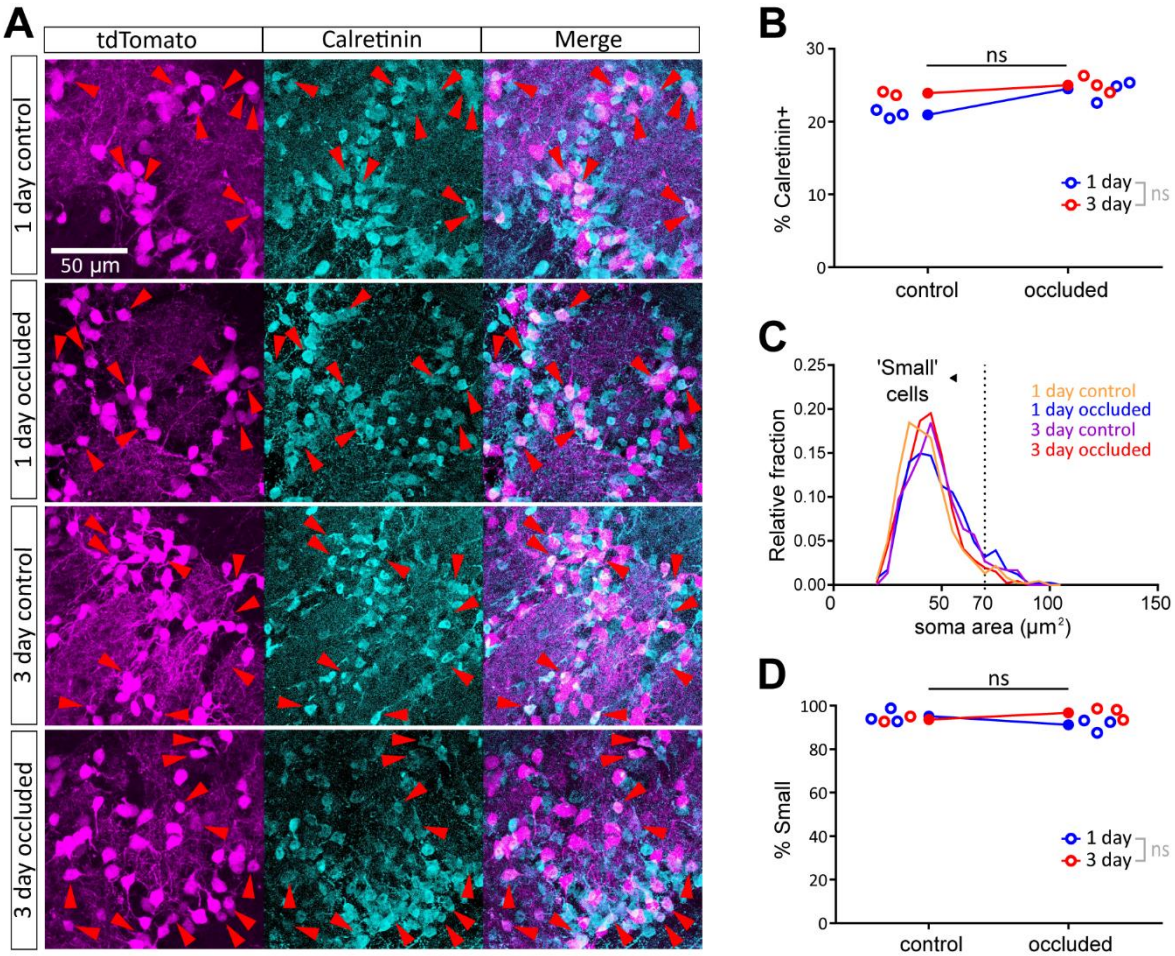

450

451 **Figure 3**. Brief naris occlusion does not alter the sub-type composition of olfactory bulb DAT-tdTomato neurons. **A)**
452 Example maximum intensity projection images showing immunofluorescence for tdTomato and calretinin in the glomerular
453 layer of the olfactory bulb in 1 and 3 day control and occluded DAT-tdTomato mice. Red arrowheads indicate example
454 neurons co-expressing DAT-tdTomato and calretinin. **B)** Line plots showing, for each treatment group, overall % of
455 tdTomato+ neurons that also express calretinin. Open circles show % values for individual mice. Fisher's exact test with
456 Bonferroni correction for multiple comparisons ($\alpha = 0.025$); ns, non-significant. **C)** Histogram of soma sizes for all
457 tdTomato+ neurons in each treatment condition. Dotted line shows 70 μm^2 threshold for cells classed as 'small'. **D)** Small
458 cell % data; all conventions as in **B**.

459

460

461 *Brief sensory deprivation does not affect GAD67 expression in olfactory bulb DAT-tdTomato neurons*

462 Having confirmed that brief unilateral naris occlusion effectively lowers activity levels in the
463 olfactory bulb DAT-tdTomato population without affecting its subtype composition, we used this
464 mouse line to investigate potential experience-dependent plasticity in the expression of
465 neurotransmitter-synthesising enzymes. We focused first on the GABA-synthesising enzyme isoform
466 GAD67, which is ubiquitously expressed in dual GABA- and dopamine-releasing olfactory bulb
467 neurons (Kosaka & Kosaka, 2007; Kiyokage *et al.*, 2010; Kosaka *et al.*, 2019), and has been previously
468 reported to undergo experience-dependent changes in both mRNA expression and protein levels
469 after prolonged manipulations (Parrish-Aungst *et al.*, 2011; Lau & Murthy, 2012; Banerjee *et al.*,
470 2013; Wang *et al.*, 2017). However, here we observed no effect of either 1 day or 3 day naris
471 occlusion on levels of *Gad1* mRNA from wild-type whole-bulb samples (Fig.4A; 1 day mean ± SEM
472 fold change: sham, 1.06 ± 0.12; occluded, 1.08 ± 0.082; t-test with $\alpha = 0.025$, $t_{18} = 0.11$, $p = 0.92$,
473 N = 20; 3 day: sham, 1.01 ± 0.041; occluded, 0.90 ± 0.061; t-test with $\alpha = 0.025$, $t_{14} = 1.45$, $p = 0.17$;
474 N = 16). We also found no changes in relative GAD67 immunofluorescence intensity in olfactory bulb
475 DAT-tdTomato neurons after 1 or 3 days of unilateral naris occlusion (Fig.4B-D; normalised
476 immunofluorescence intensity (%) mean ± SEM: 1 day control, 97.43 ± 3.08 %, n = 261, N = 3; 1 day
477 occluded, 92.93 ± 2.89 %, n = 314, N = 3; 3 day control, 103.50 ± 3.70 %, n = 192, N = 2; 3 day
478 occluded, 94.03 ± 2.88 %, n = 304, N = 3. Multi-level ANOVA controlling for set variance, effect of
479 manipulation, $F_{1,1071} = 0.089$, $p = 0.77$; effect of time, $F_{1,1071} = 1.60$, $p = 0.21$; effect of manipulation x
480 time interaction, $F_{1,1071} = 0.62$, $p = 0.43$).

481

482 **Figure 4**

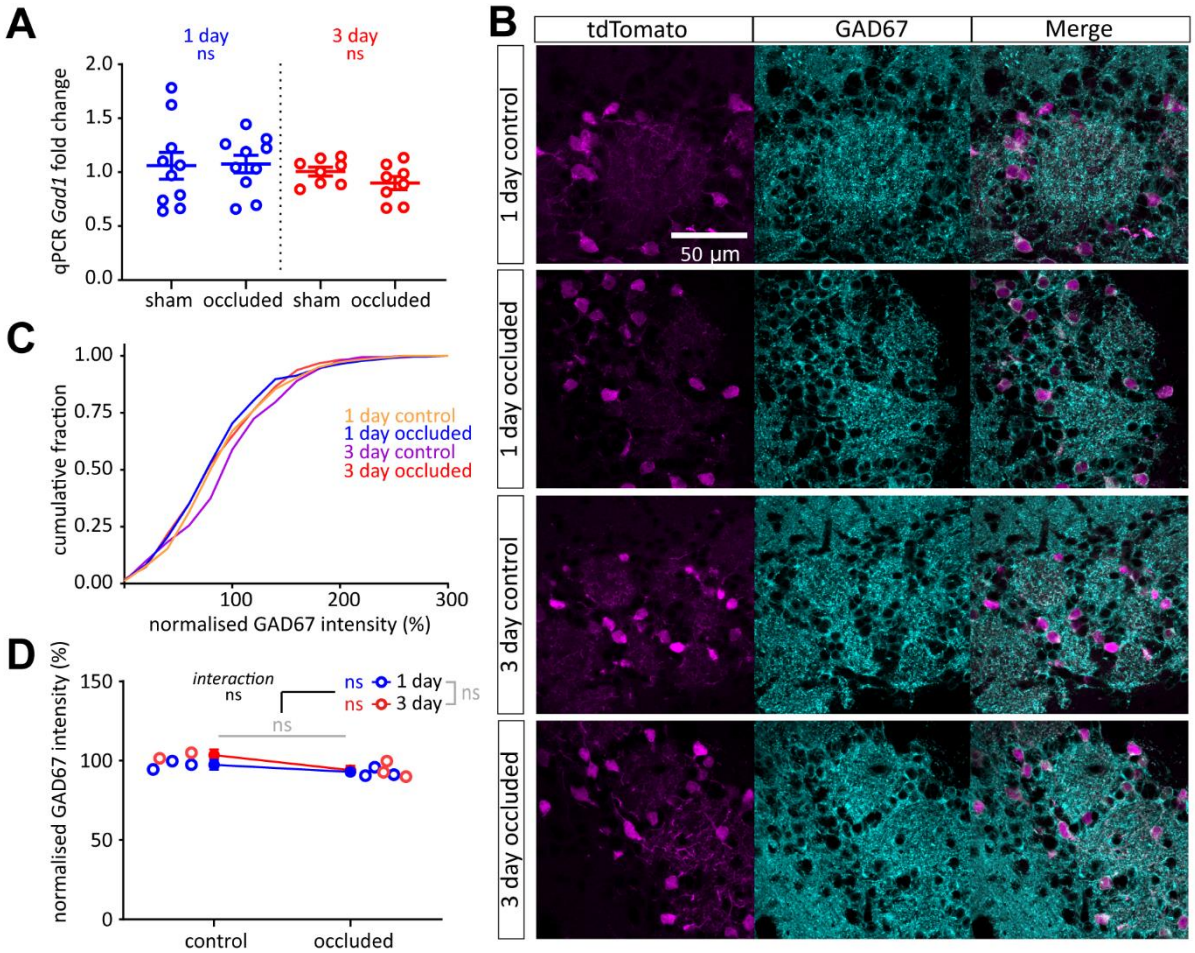

483

484 **Figure 4**. Brief sensory deprivation does not affect GAD67 expression in olfactory bulb DAT- tdTomato neurons. **A)** *Gad1*
485 mRNA expression by whole-bulb qPCR. Circles show fold change for individual bulbs vs relevant sham control mean; lines
486 show mean ± SEM fold change for each group. **B)** Example maximum intensity projection images showing
487 immunofluorescence for GAD67 in the glomerular layer of the olfactory bulb in 1 and 3 day control and occluded DAT-
488 tdTomato mice. All images are from the same co-embedded preparation, acquired and presented with identical settings.
489 **C)** Cumulative distribution of normalised GAD67 intensity (%) in DAT-tdTomato neurons in each treatment group. **D)** Line
490 plots showing overall mean ± SEM of normalised GAD67 intensity (%) in each treatment group; unfilled circles show mean
491 normalised GAD67 intensity (%) for individual mice. Multi-level ANOVA controlling for set variance; effect of manipulation
492 and effect of time, ns: non-significant.

493

494

495 *DDC expression in olfactory bulb DAT-tdTomato neurons is only slightly and transiently reduced by*
496 *unilateral naris occlusion*

497 The enzyme DDC catalyses the direct synthesis of dopamine from L-DOPA, but unlike TH has
498 received relatively little attention regarding its potential for activity-dependent expression. Indeed,
499 two previous studies found no effect of odour deprivation on *Ddc* mRNA levels in the olfactory bulb
500 following prolonged, >1 month-long naris closure (Stone *et al.*, 1990; Cave *et al.*, 2010). Here, in
501 whole-bulb samples from wild-type mice, we observed a trend towards increased *Ddc* mRNA levels
502 after 1 day naris occlusion, but no effect of sensory deprivation at the longer, 3 day interval (Fig.5A;
503 1 day mean ± SEM fold change: sham, 1.08 ± 0.11; occluded, 1.35 ± 0.099; t-test with $\alpha = 0.025$,
504 $t_{27} = 1.81$, $p = 0.081$, N = 29; 3 day: sham, 1.03 ± 0.11; occluded, 1.14 ± 0.16; t-test with $\alpha = 0.025$,
505 $t_{14} = 0.52$, $p = 0.61$; N = 16). In contrast, examining relative DDC immunofluorescence intensity
506 specifically in olfactory bulb DAT-tdTomato neurons revealed a very small but nevertheless
507 significant *decrease* after naris occlusion. (Fig. 5B-D; normalised immunofluorescence intensity (%)
508 mean ± SEM: 1 day control, 99.65 ± 1.44%, n = 884, N = 4; 1 day occluded, 92.17 ± 1.51%, n = 841, N
509 = 4; 3 day control, 100.51 ± 1.48%, n = 609, N = 3; 3 day occluded, 98.56 ± 1.53%, n = 819, N = 4.
510 Multi-level ANOVA controlling for set variance, effect of manipulation, $F_{1,3152} = 10.62$, $p = 0.0010$;
511 effect of time, $F_{1,3097} = 0.00$, $p = 0.99$; effect of manipulation x time interaction, $F_{1,3140} = 4.75$, $p =$
512 0.029). The significant manipulation-by-time interaction here was supported by pairwise post-hoc
513 tests demonstrating that this effect was driven by a significant reduction in DDC
514 immunofluorescence only after 1 day of occlusion, with expression of DDC in 3 day occluded DAT-
515 tdTomato neurons then returning back to control levels (Fig. 5D; Bonferroni post- test comparing
516 control versus occluded with $\alpha = 0.025$: 1 day, $F_{1,1722} = 11.84$, $p < 0.0001$; 3 day, $F_{1,738} = 0.59$, $p =$
517 0.44). Small and transient changes in relative DDC levels are therefore possible in olfactory bulb
518 dopaminergic cells experiencing sustained decreases in activity.

519

520 **Figure 5**

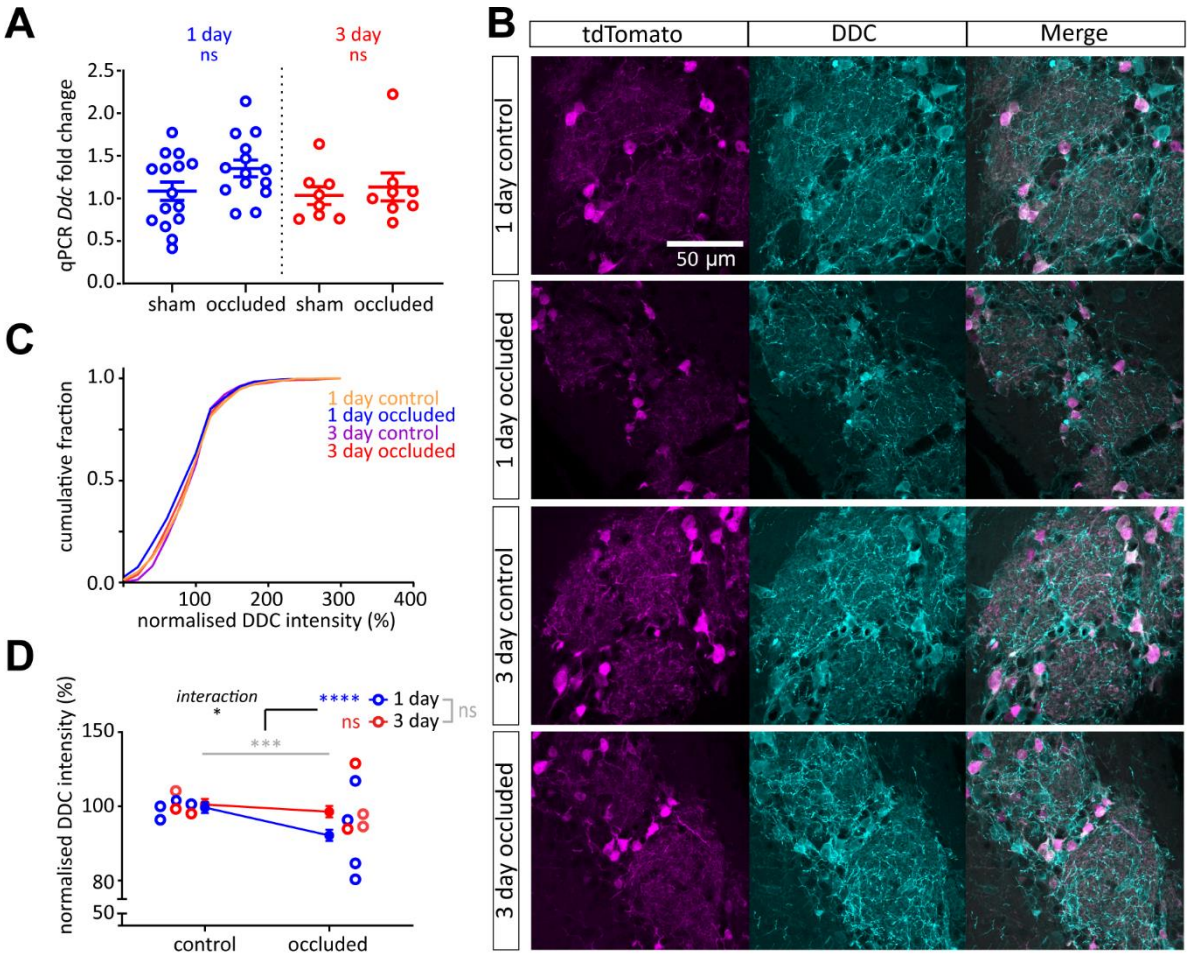

521

522 **Figure 5**. DDC expression in olfactory bulb DAT-tdTomato neurons is slightly reduced only after 1 day of unilateral naris
523 occlusion. **A)** *Ddc* mRNA expression by whole-bulb qPCR. Circles show fold change for individual bulbs vs relevant sham
524 control mean; lines show mean ± SEM fold change for each group. **B)** Example maximum intensity projection images
525 showing immunofluorescence for DDC in the glomerular layer of the olfactory bulb in 1 and 3 day control and occluded
526 DAT-tdTomato mice. All images are from the same co-embedded preparation, acquired and presented with identical
527 settings. **C)** Cumulative distribution of normalised DDC intensity (%) in DAT-tdTomato neurons in each treatment group.
528 **D)** Line plots showing overall mean ± SEM of normalised DDC intensity (%) in each treatment group; unfilled circles show
529 mean normalised DDC intensity (%) for individual mice. Multi-level ANOVA controlling for set variance; effect of
530 manipulation, *** $p < 0.001$; effect of time, ns: non-significant; effect of interaction, * $p < 0.05$. Bonferroni post-test
531 ($\alpha = 0.025$); 1 day, effect of manipulation, **** $p < 0.0001$; 3 day, effect of manipulation, ns: non-significant.

532

533

534 *Brief sensory deprivation reduces TH expression in olfactory bulb DAT-tdTomato neurons*

535 Olfactory bulb dopaminergic neurons have a well-described ability to regulate TH expression in an
536 activity-dependent manner, including after unilateral naris occlusion by plug insertion (Nadi *et al.*,
537 1981; Baker *et al.*, 1983; Kosaka *et al.*, 1987; Cummings *et al.*, 1997). At the mRNA level, plasticity in
538 *Th* expression has been previously reported after 2 days of odour deprivation (Cho *et al.*, 1996). Here
539 we also observed rapid occlusion-induced downregulation of *Th* mRNA levels, as assessed via qPCR
540 on whole-bulb samples from wild-type mice. Compared to sham-treated bulbs, OBs on the occluded
541 side had significantly lower levels of *Th* expression after both 1 day and 3 days of sensory deprivation
542 (Fig.6A; 1 day mean ± SEM fold change: sham, 1.02 ± 0.049; occluded, 0.64 ± 0.030; t-test with
543 $\alpha = 0.025$, $t_{27} = 6.55$, $p < 0.0001$, N = 29; 3 day: sham, 1.04 ± 0.13; occluded, 0.53 ± 0.029; Welch's t-
544 test with $\alpha = 0.025$, $t_{7.73} = 4.00$, $p = 0.0043$; N = 16).

545 At the protein level, just one day of elevated activity in cultured bulbar neurons or slices has been
546 found to increase TH immunofluorescence intensity or TH-GFP transgene expression (Akiba *et al.*,
547 2007; Chand *et al.*, 2015). We also recently found that 24 h naris occlusion was accompanied by a
548 significant drop in immunofluorescence for TH in the ipsilateral olfactory bulb, without producing a
549 change in TH-positive cell density (Galliano et al., 2021). However, the above approaches had the
550 drawback that they used TH expression itself as a means to identify samples for TH quantification.
551 We therefore used our conditional genetic labelling strategy to assess rapid deprivation-induced
552 changes in TH expression in an independently identified neuronal population.

553 Brief sensory deprivation was indeed associated with a decrease in the relative intensity of TH
554 immunofluorescence in olfactory bulb DAT tdTomato neurons (Fig.6B-D; normalised
555 immunofluorescence intensity (%) mean ± SEM: 1 day control, 95.27 ± 3.35%, n = 460, N = 3; 1 day
556 occluded, 70.96 ± 3.16%, n = 408, N = 3; 3 day control, 107.30 ± 4.64%, n = 298, N = 2; 3 day
557 occluded, 57.00 ± 2.32%, n = 461, N = 3. Multi-level ANOVA controlling for set variance, effect of
558 manipulation, $F_{1,1546.} = 2.90$, $p = 0.089$; effect of time, $F_{1,1626} = 3.10$, $p = 0.078$). This effect was highly
559 significant after just 1 day (Fig. 6C; Bonferroni post-test comparing control versus occluded with
560 $\alpha = 0.025$: 1 day, $F_{1,867} = 27.41$, $p < 0.00005$), but was even stronger after 3 days (Fig. 6C; post-test: 3
561 day, $F_{1,639} = 76.36$, $p < 0.00005$; effect of manipulation x time interaction in main ANOVA, $F_{1,1613} =$
562 11.67, $p = 0.001$). Continuous naris occlusion therefore produces a rapid downregulation in TH
563 immunofluorescence in independently identified olfactory bulb dopaminergic neurons, and this
564 effect becomes stronger over time.

565

566

567 **Figure 6**

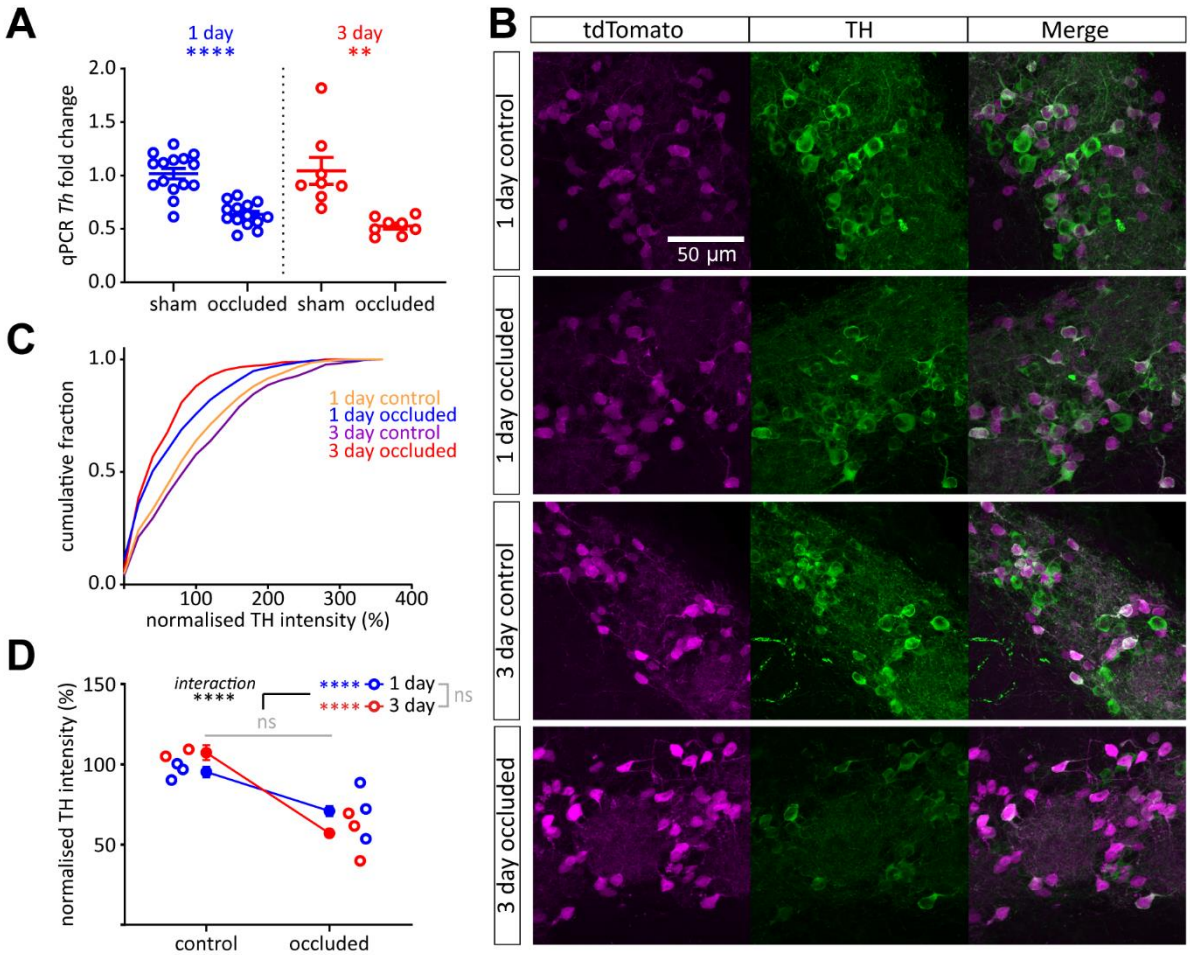

568

569 **Figure 6**. Brief sensory deprivation reduces TH expression in olfactory bulb DAT-tdTomato neurons. **A)** *Th* mRNA
570 expression by whole-bulb qPCR. Circles show fold change for individual bulbs vs relevant sham control mean; lines show
571 mean ± SEM fold change for each group. t-test (α = 0.025); 1 day, ****, $p < 0.0001$; 3 day, **, $p = 0.0043$. **B)** Example
572 maximum intensity projection images showing immunofluorescence for TH in the glomerular layer of the olfactory bulb in
573 1 and 3 day control and occluded DAT-tdTomato mice. All images are from the same co-embedded preparation, acquired
574 and presented with identical settings. **C)** Cumulative distribution of normalised TH intensity (%) in DAT-tdTomato neurons
575 in each treatment group. **D)** Line plots showing overall mean ± SEM of normalised TH intensity (%) in each treatment
576 group; unfilled circles show mean normalised TH intensity (%) for individual mice. Multi-level ANOVA controlling for set
577 variance; effect of manipulation x time interaction, **** $p < 0.0001$; effect of manipulation and effect of time, ns: non-
578 significant. Bonferroni post-test (α = 0.025); 1 day, effect of manipulation, **** $p < 0.00005$; 3 day, effect of manipulation,
579 **** $p < 0.00005$.

580

581

582 **Discussion**

583

584 Here we used a conditional genetic strategy to identify olfactory bulb neurons expressing the
585 dopamine transporter. DAT-tdTomato neurons were predominantly dopaminergic, but also included
586 a subset of non-dopaminergic, calretinin-positive cells. Importantly, while cFos immunolabel
587 showed that the activity of DAT-tdTomato cells could be readily manipulated with brief periods of
588 sensory deprivation, these manipulations did not alter the labelled neurons' subtype composition.
589 We found that 1-3 days of unilateral naris occlusion was insufficient to alter expression of the GABA-
590 synthesising enzyme GAD67 in these cells. In contrast, similarly brief sensory manipulations were
591 associated with significant activity-dependent changes in the levels of enzymes required for the
592 synthesis of dopamine.

593

594 *Identifying olfactory bulb dopaminergic neurons using DAT$^{IRES\mathrm{cre}}$ mice*

595 Using transgenic approaches to label specific cell types in the brain requires thorough
596 characterisation of their specificity. To specifically label dopaminergic neurons in the olfactory
597 bulb's glomerular layer, several previous studies have successfully utilised conditional or knock-in
598 strategies based on expression driven from the *Th* promoter (e.g. Saino-Saito *et al.*, 2004; Pignatelli
599 *et al.*, 2005; Kiyokage *et al.*, 2010; Adam & Mizrahi, 2011; Liu *et al.*, 2013; Wachowiak *et al.*, 2013).
600 However, this approach can also result in labelled presumptive immature migrating neurons outside
601 the glomerular layer, which can express *Th* mRNA before TH protein expression is detectable (Saino-
602 Saito *et al.*, 2004; Pignatelli *et al.*, 2009; Banerjee *et al.*, 2013). We therefore opted for a different
603 conditional genetic labelling strategy based on Cre recombinase expression under the control of the
604 DAT promoter, which has been reported to be specific to TH-positive neurons in general (Lammel *et*
605 *al.*, 2015), and which has already been used successfully to target olfactory bulb dopaminergic
606 neurons. In those bulb studies, which either employed the DAT$^{IRES\mathit{cre}}$ line used here (Vaaga *et al.*,
607 2017; Short & Wachowiak, 2019; Sato *et al.*, 2020) a DAT-Cre knock-in model (Ninkovic *et al.*, 2010;
608 Banerjee *et al.*, 2015), or a BAC transgenic DAT-CreER^{T2} inducible line (Bywalez *et al.*, 2016),
609 approximately 85% of genetically-labelled neurons were found to be TH-positive by
610 immunohistochemistry (Banerjee *et al.*, 2015; Vaaga *et al.*, 2017). This is broadly in line with the
611 ~75% co-label we found here, with cross-study variability possibly arising from differences in the
612 Cre-dependent reporter lines utilised and/or differences in label detection criteria. Nevertheless,

613 the general approach of using DAT-Cre mice to label dopaminergic neurons in the olfactory bulb
614 clearly produces reasonable specificity.

615 However, we found that not all DAT-tdTomato olfactory bulb cells were TH-positive, and that the
616 large majority of non-dopaminergic genetically labelled neurons (~20 %) expressed the calcium-
617 binding protein calretinin. Calretinin expression in DAT-Cre-positive bulbar neurons has been
618 previously reported, but not quantified, in a separate knock-in line (Ninkovic *et al.*, 2010). This
619 suggests that off-target label of calretinin cells is not a peculiarity of one particular genetic
620 manipulation, but instead reflects a biological link between these neurons and their dopaminergic
621 neighbours. Indeed, fate mapping neuronal precursors that generate glomerular layer GABAergic
622 interneurons has demonstrated that the decision to differentiate into a dopaminergic neuron over a
623 calretinin neuron relies on just a few transcription factors. Loss of Pax6, Dlx2 or Meis2 reduces the
624 proportion of postnatal dopaminergic neurons that are generated, while increasing the number of
625 calretinin neurons (Brill *et al.*, 2008; Agoston *et al.*, 2014). Overexpression of Dlx2 increases the
626 proportion of dopaminergic neurons and decreases the calretinin population (Brill *et al.*, 2008). The
627 transcription factor Er81 is also expressed in both calretinin and dopaminergic neurons in the
628 glomerular layer and is important in mice for regulating the expression of *Th* (Cave *et al.*, 2010).
629 Therefore, the molecular determinants of dopaminergic versus calretinin identities appear to be
630 closely interdependent. It remains unclear whether tdTomato expression in some calretinin neurons
631 is due to transient expression of DAT during their development, or whether this subset of cells
632 continues to express DAT postnatally. In the former case, obtaining transgenic label via inducible
633 activation of DAT-Cre in mature mice (Bywalez *et al.*, 2016) might result in greater specificity for
634 bulbar dopaminergic neurons. Low levels of bulbar DAT expression (Cockerham *et al.*, 2016)
635 unfortunately precluded us from addressing this question using immunohistochemistry, but targeted
636 interrogation of single-cell sequencing datasets (e.g. Zeisel *et al.*, 2018) might provide an answer in
637 the near future. Regardless, it is clear that this minority calretinin-expressing population needs to be
638 considered when interpreting the results of experiments performed on 'dopaminergic' neurons
639 targeted via DAT-Cre mouse lines (Wachowiak *et al.*, 2013; Banerjee *et al.*, 2015; Bywalez *et al.*,
640 2016; Vaaga *et al.*, 2017; Galliano *et al.*, 2018, 2020; Sato *et al.*, 2020). Thankfully, though, the
641 distinct and unusually immature-like properties of glomerular layer calretinin-positive cells, including
642 their extremely low excitability and apparent lack of GABA release (Fig. 1G; Fogli Iseppe *et al.*, 2016;
643 Benito *et al.*, 2018; Tavakoli *et al.*, 2018), mean that their presence as a minority of DAT-Cre-targeted
644 cells is unlikely to have significantly biased the conclusions of those previous studies.

645 Our main goal was to achieve reasonable specificity in genetically labelling olfactory bulb
646 dopaminergic neurons, but we note that our approach was by no means comprehensive in labelling

647 *all* olfactory bulb dopaminergic neurons. As is the case for many Cre lines (Heffner *et al.*, 2012), we
648 saw mosaicism in the fact that many immunohistochemically-defined TH-positive neurons did not
649 express the tdTomato marker (see Fig. 1B,E; % of TH-positive neurons that were tdTomato-negative,
650 36 ± 0.2 %, n = 692 cells, N = 3 mice; Galliano *et al.*, 2018). The DAT$^{IRES\mathit{cre}}$ line is also known to
651 particularly under-represent one subtype of bulbar dopaminergic neuron – the large-soma, axon-
652 bearing, embryonically-generated subclass (Galliano *et al.*, 2018) – and we found again here that
653 small-soma, presumed anaxonic neurons dominate the tdT-labelled population. However, large-
654 soma, axon-positive cells are already rare amongst the olfactory bulb dopaminergic population, and
655 they can certainly still be labelled in DAT-tdTomato mice (Galliano *et al.*, 2018). So, although the
656 DAT$^{IRES\mathit{cre}}$ line produces genetic label which is heavily biased towards one particular dopaminergic
657 subpopulation in the olfactory bulb, it is far from being entirely subtype specific. Overall, the
658 strategy of using DAT-based transgenic lines to target dopaminergic neurons in the olfactory bulb
659 can produce good levels of specificity, but care needs to be taken to fully characterise the resulting
660 label before such experiments can be safely interpreted.

661

662 *Experience-dependent plasticity of GAD67*

663 With brief periods of sensory deprivation, we saw no evidence here for changes in relative GAD67
664 immunofluorescence amongst olfactory bulb DAT-tdTomato-expressing neurons. Given the mixed
665 calretinin- and TH-positive composition of our tdTomato-labelled population (Fig. 1), this result could
666 theoretically have been produced if changes in GAD67 levels in dopaminergic neurons were
667 perfectly offset by inverse, and stronger, changes in the smaller calretinin-positive tdTomato
668 subgroup. However, such effects might be expected to significantly change the shape of the
669 distribution of GAD67 relative immunofluorescence values, and we saw no obvious changes of this
670 nature in our data (Fig.4C). We did not co-label for calretinin and GAD67 in this study, while the
671 literature contains conflicting reports as to whether calretinin-positive neurons in the olfactory bulb
672 express GAD67 at all (Panzanelli *et al.*, 2007; Parrish-Aungst *et al.*, 2007; opposing results are likely
673 due to the different transgenic versus immunohistochemical labelling methods employed in these
674 studies). Even if calretinin-positive tdTomato cells do express GAD67, however, the most
675 parsimonious interpretation of our data remains that dopaminergic bulbar neurons do not rapidly
676 alter their GAD67 levels in response to sensory deprivation. This fits with previous work measuring
677 general GAD (i.e. GAD65+67) expression in the bulb, which found no significant alterations following
678 more long-term sensory deprivation (Kosaka *et al.*, 1987; Stone *et al.*, 1991; Baker *et al.*, 1993). In
679 contrast, reduced expression of GAD67, but not GAD65, has been observed after 7 days of unilateral

680 naris occlusion and deafferentation via measures of glomerular layer immunofluorescence and
681 whole-bulb protein expression (Parrish-Aungst *et al.*, 2011). Decreased expression of *Gad1* mRNA
682 and GAD67 protein have also been described following chemical ablation of olfactory sensory
683 neurons (Lau & Murthy, 2012) or unilateral naris occlusion (Banerjee *et al.*, 2013; Wang *et al.*, 2017).
684 However, these studies used longer-duration manipulations and did not distinguish between
685 different bulbar neuronal populations. Therefore, either 1-3 days of unilateral naris occlusion is
686 insufficient to induce activity dependent changes in GAD67, or measures based on
687 immunofluorescence intensity may not be sensitive enough to always detect changes in GAD67, or
688 these changes are driven in neurons not labelled in the DAT-tdTomato mouse line.

689

690 *Experience-dependent plasticity of dopamine-synthesising enzymes*

691 We report here the first evidence for an activity-dependent change in olfactory bulb DDC levels. This
692 effect was very small and only transient, with relative DDC immunofluorescence in DAT-tdTomato
693 neurons decreasing slightly after 1 day of naris occlusion and returning back to baseline after just
694 3 days of sensory deprivation. It was also in the opposite direction to the trend we observed in
695 whole-bulb qPCR data, which suggested a transient *increase* in *Ddc* mRNA after 1 day occlusion.
696 Perhaps this mRNA increase reflects a transcriptional rebound already in operation after just 24 h
697 deprivation, driving DDC protein rapidly back towards control levels. The small and temporary
698 experience-dependent DDC immunofluorescence alteration we observed might explain why
699 previous studies of potential bulbar DDC plasticity – which used much longer periods of sensory
700 manipulation - did not find similar effects (Stone *et al.*, 1990; Cave *et al.*, 2010). However, expression
701 of DDC in the midbrain has been reported to be affected within a few hours of activation or blockade
702 of dopamine receptors (Hadjiconstantinou *et al.*, 1993; Zhu *et al.*, 1993). Further work is needed to
703 confirm whether downregulation of bulbar DDC after 1 day of occlusion is a consistent activity-
704 dependent modification. If so, it might reflect an initial strategy whereby dopaminergic neurons
705 downregulate multiple nodes in the dopamine synthesis pathway, before sufficiently decreased TH
706 activity can alone – as the rate-limiting step – control levels of transmitter production.

707 Our data showing decreased TH expression after olfactory sensory deprivation are entirely
708 consistent with a large body of prior work describing this effect (Nadi *et al.*, 1981; Baker *et al.*, 1983,
709 1984, 1993, 1999; Kosaka *et al.*, 1987; Baker, 1990; Stone *et al.*, 1990; Cho *et al.*, 1996; Philpot *et al.*,
710 1998; Saino-Saito *et al.*, 2004; Bastien-Dionne *et al.*, 2010; Cave *et al.*, 2010; Weiss *et al.*, 2011; Grier
711 *et al.*, 2016), including some indications that it can occur after relatively brief manipulations (Cho *et*
712 *al.*, 1996; Akiba *et al.*, 2007; Chand *et al.*, 2015; Galliano et al., 2021). It is novel, however, that our

713 methodological approach demonstrated activity-dependent TH alterations in cells identified in an
714 entirely TH-independent manner. As discussed above, this approach was not completely selective,
715 labelling a minority of calretinin-positive neurons in addition to dopaminergic cells. However, since
716 we never observed a DAT-tdTomato neuron that was both calretinin-positive and dopaminergic, and
717 since the proportions of calretinin-positive cells did not change significantly with occlusion (Fig. 3),
718 this off-target labelled sub-population cannot account for the relative changes in TH and DDC
719 immunofluorescence we observed. Indeed, if anything, the presence of a significant proportion of
720 essentially TH- or DDC-negative cells amongst the DAT-tdTomato samples we analysed may have
721 made our ability to detect relative differences in enzyme levels less sensitive.

722 We also note the caveat that, of course, changes in immunofluorescence intensity cannot be used to
723 infer activity-dependent plasticity in *absolute* levels of protein expression. With this approach,
724 results can be easily confounded by variability in the duration of immunohistochemistry steps, the
725 composition of reagents, and/or individual image acquisition settings. We did take every possible
726 measure to mitigate against such factors, comparing tissue from mice that were fixed on the same
727 day with the same fixative solution, comparing sections that were physically co-embedded prior to
728 all stages of histological processing, and comparing images that were taken on the same day with
729 the same acquisition settings. We also ensured that we only ever made *relative* comparisons of
730 immunofluorescence. So, while we are confident that, for example, TH levels decreased in DAT-
731 tdTomato cells after 1 day of sensory deprivation, we do not claim any insight into the magnitude of
732 this decrease. We do, however, have corroborative, fully quantitative qPCR data to show that – at
733 least at the whole-bulb level – brief sensory deprivation is associated with an approximate halving of
734 *Th* mRNA levels.

735

736 *Mechanisms*

737 It remains unclear precisely how activity-dependent changes in TH expression occur, though the
738 immediate depolarisation-activated pathways appear to require signalling through L-type CaV1
739 Channels and cAMP (Cigola *et al.*, 1998), and *Th* gene expression is at least partly controlled by
740 changes in secondary DNA structure influencing the binding of heterogeneous nuclear
741 ribonucleoproteins (hnRNPs) to its proximal promoter (Banerjee *et al.*, 2014; Wang *et al.*, 2017). Our
742 findings suggest that these processes can work over reasonably quick timescales. However, given
743 the similarity in promoter-based changes in secondary structure and hnRNP binding between the *Th*
744 and *Gad1* genes (Wang et al., 2017), it will be interesting to consider how these processes can work
745 more rapidly, more specifically, and/or be coupled with targeted changes in mRNA and protein

746 turnover, to produce selective downregulation of TH without any changes in GAD67 after a few days
747 of naris occlusion.

748

749 *Implications for sensory processing*

750 Plasticity of TH expression is believed to be a way in which the olfactory bulb can tune its levels of
751 dopaminergic signalling according to changes in incoming sensory-evoked activity. Given some of
752 the known effects of dopamine in glomerular networks, this could potentially have the effect of
753 counteracting input activity perturbation. For example, the best-described circuit-level effect of
754 dopamine in the bulb is its inhibitory action on the release of glutamate from olfactory sensory
755 neuron axon terminals, which it achieves via D2 receptor activation (Hsia *et al.*, 1999; Berkowicz &
756 Trombley, 2000; Ennis *et al.*, 2001; Maher & Westbrook, 2008; McGann, 2013; Vaaga *et al.*, 2017). If
757 sensory input levels are chronically decreased, it might be adaptive to reduce the strength of this
758 inhibition, perhaps by decreasing expression of the rate-limiting enzyme for neurotransmitter
759 synthesis. This might put the system into a state of higher-gain readiness for the low levels of input
760 that will initially arrive if and when sensory stimulation recommences. Indeed, the volume-
761 transmission nature of sensory neuron presynaptic inhibition (Pinching & Powell, 1971; McGann,
762 2013), coupled with the high threshold and slow dynamics of bulbar dopamine release (Borisovska *et*
763 *al.*, 2013), might make for a slow modulatory process that is well suited to days-scale modification
764 via plasticity of enzyme expression. However, given the strong presynaptic inhibition also mediated
765 by $GABA_B$ receptor activation on OSN terminals (McGann, 2013), it is unclear why dopamine- but not
766 GABA-synthesising enzymes are targets for rapid activity-dependent regulation in this circuit. It may
767 be that GABAergic inhibition is modulated by distinct plastic mechanisms that do not target
768 transmitter synthesis. Alternatively, distinct mechanisms of GABAergic and dopaminergic inhibition
769 that can occur within the same presynaptic terminals (Burke *et al.*, 2018) might be individually tuned
770 according to sensory experience.

771 In contrast, the potential functional implications of TH plasticity on the less-understood postsynaptic
772 effects of bulbar dopamine transmission are harder to predict. Dopamine can act via D1-type
773 receptors to promote rebound firing after interglomerular GABAergic inhibition of external tufted
774 cells (Liu *et al.*, 2013), so perhaps decreased TH levels might lead to more prolonged lateral
775 inhibition within the glomerular layer. The implications of such an effect for information processing
776 in sensory-deprived bulbar circuits might be best addressed via computational network modelling.
777 Most important, though, is the fact that, although experience-dependent plasticity in olfactory bulb
778 TH expression has been described for decades, it is still not known how (or whether) changes in TH

779 mRNA and protein levels give rise to alterations in the amount of dopamine actually released.
780 Future experiments should be able to control the activity of dopaminergic neurons whilst monitoring
781 the resulting effects of dopamine release (e.g. Vaaga *et al.*, 2017), in order to quantitatively compare
782 the outcome in control versus sensory-deprived tissue.

Author Contributions

DJB, ML & MG designed experiments; DJB, AC & ML performed experiments; DJB, ML & MG analysed data; DJB, ML & MG wrote the paper.

Conflict of Interest

The authors declare no conflicts of interest.

Acknowledgements

This work was supported by a Medical Research Council 4-year PhD studentship to DJB, and a Leverhulme Trust Research Grant (RPG-2016-095) and ERC Consolidator Grant (725729; FUNCOPLAN) to MSG. We wish to thank Beatriz Rico for access to equipment, Laura Andreae and Elisa Galliano for comments on the manuscript, and Elisa Galliano, Christiane Hahn and other past and present members of the Grubb laboratory for technical assistance and stimulating discussion.

Data accessibility

The data that support the findings of this study will be fully and openly available upon publication in a public repository that issues datasets with DOIs.

807 **References**

808 Adam, Y. & Mizrahi, A. (2011) Long-term imaging reveals dynamic changes in the neuronal
809 composition of the glomerular layer. *J. Neurosci.*, **31**, 7967–7973.
810 Agoston, Z., Heine, P., Brill, M.S., Grebbin, B.M., Hau, A.-C., Kallenborn-Gerhardt, W., Schramm, J.,
811 Götz, M., & Schulte, D. (2014) Meis2 is a Pax6 co-factor in neurogenesis and dopaminergic
812 periglomerular fate specification in the adult olfactory bulb. *Development*, **141**, 28–38.
813 Akiba, Y., Sasaki, H., Saino-Saito, S., & Baker, H. (2007) Temporal and spatial disparity in cFOS
814 expression and dopamine phenotypic differentiation in the neonatal mouse olfactory bulb.
815 *Neurochem. Res.*, **32**, 625–634.
816 Bäckman, C.M., Malik, N., Zhang, Y., Shan, L., Grinberg, A., Hoffer, B.J., Westphal, H., & Tomac, A.C.
817 (2006) Characterization of a mouse strain expressing Cre recombinase from the 3'
818 untranslated region of the dopamine transporter locus. *Genesis*, **44**, 383–390.
819 Baker, H. (1990) Unilateral, neonatal olfactory deprivation alters tyrosine hydroxylase expression but
820 not aromatic amino acid decarboxylase or GABA immunoreactivity. *Neuroscience*, **36**, 761–
821 771.
822 Baker, H., Cummings, D.M., Munger, S.D., Margolis, J.W., Franzen, L., Reed, R.R., & Margolis, F.L.
823 (1999) Targeted deletion of a cyclic nucleotide-gated channel subunit (OCNC1): biochemical
824 and morphological consequences in adult mice. *J. Neurosci.*, **19**, 9313–9321.
825 Baker, H., Kawano, T., Albert, V., Joh, T.H., Reis, D.J., & Margolis, F.L. (1984) Olfactory bulb dopamine
826 neurons survive deafferentation-induced loss of tyrosine hydroxylase. *Neuroscience*, **11**,
827 605–615.
828 Baker, H., Kawano, T., Margolis, F.L., & Joh, T.H. (1983) Transneuronal regulation of tyrosine
829 hydroxylase expression in olfactory bulb of mouse and rat. *J. Neurosci.*, **3**, 69–78.
830 Baker, H., Morel, K., Stone, D.M., & Maruniak, J.A. (1993) Adult naris closure profoundly reduces
831 tyrosine hydroxylase expression in mouse olfactory bulb. *Brain Res.*, **614**, 109–116.
832 Banerjee, A., Marbach, F., Anselmi, F., Koh, M.S., Davis, M.B., Garcia da Silva, P., Delevich, K., Oyibo,
833 H.K., Gupta, P., Li, B., & Albeanu, D.F. (2015) An Interglomerular Circuit Gates Glomerular
834 Output and Implements Gain Control in the Mouse Olfactory Bulb. *Neuron*, **87**, 193–207.
835 Banerjee, K., Akiba, Y., Baker, H., & Cave, J.W. (2013) Epigenetic control of neurotransmitter
836 expression in olfactory bulb interneurons. *Int. J. Dev. Neurosci.*, **31**, 415–423.
837 Banerjee, K., Wang, M., Cai, E., Fujiwara, N., Baker, H., & Cave, J.W. (2014) Regulation of tyrosine
838 hydroxylase transcription by hnRNP K and DNA secondary structure. *Nat Commun*, **5**, 5769.
839 Bastien-Dionne, P.-O., David, L.S., Parent, A., & Saghatelyan, A. (2010) Role of sensory activity on
840 chemospecific populations of interneurons in the adult olfactory bulb. *J. Comp. Neurol.*, **518**,
841 1847–1861.
842 Benito, N., Gaborieau, E., Sanz Diez, A., Kosar, S., Foucault, L., Raineteau, O., & De Saint Jan, D.
843 (2018) A Pool of Postnatally Generated Interneurons Persists in an Immature Stage in the
844 Olfactory Bulb. *J. Neurosci.*, **38**, 9870–9882.
845 Berkowicz, D.A. & Trombley, P.Q. (2000) Dopaminergic modulation at the olfactory nerve synapse.
846 *Brain Res.*, **855**, 90–99.
847 Borisovska, M., Bensen, A.L., Chong, G., & Westbrook, G.L. (2013) Distinct modes of dopamine and
848 GABA release in a dual transmitter neuron. *J. Neurosci.*, **33**, 1790–1796.
849 Brill, M.S., Snapyan, M., Wohlfrom, H., Ninkovic, J., Jawerka, M., Mastick, G.S., Ashery-Padan, R.,
850 Saghatelyan, A., Berninger, B., & Götz, M. (2008) A dlx2- and pax6-dependent transcriptional
851 code for periglomerular neuron specification in the adult olfactory bulb. *J. Neurosci.*, **28**,
852 6439–6452.
853 Burke, K.J., Keeshen, C.M., & Bender, K.J. (2018) Two Forms of Synaptic Depression Produced by
854 Differential Neuromodulation of Presynaptic Calcium Channels. *Neuron*, **99**, 969-984.e7.
855 Bustin, S.A., Benes, V., Garson, J.A., Hellemans, J., Huggett, J., Kubista, M., Mueller, R., Nolan, T.,
856 Pfaffl, M.W., Shipley, G.L., Vandesompele, J., & Wittwer, C.T. (2009) The MIQE guidelines:

857 minimum information for publication of quantitative real-time PCR experiments. *Clin. Chem.*,
858 **55**, 611–622.
859 Bywalez, W.G., Ona-Jodar, T., Lukas, M., Ninkovic, J., & Egger, V. (2016) Dendritic Arborization
860 Patterns of Small Juxtaglomerular Cell Subtypes within the Rodent Olfactory Bulb. *Front*
861 *Neuroanat*, **10**, 127.
862 Cave, J.W., Akiba, Y., Banerjee, K., Bhosle, S., Berlin, R., & Baker, H. (2010) Differential regulation of
863 dopaminergic gene expression by Er81. *J. Neurosci.*, **30**, 4717–4724.
864 Chand, A.N., Galliano, E., Chesters, R.A., & Grubb, M.S. (2015) A distinct subtype of dopaminergic
865 interneuron displays inverted structural plasticity at the axon initial segment. *J. Neurosci.*,
866 **35**, 1573–1590.
867 Cheetham, C.E.J., Park, U., & Belluscio, L. (2016) Rapid and continuous activity-dependent plasticity
868 of olfactory sensory input. *Nat Commun*, **7**, 10729.
869 Cho, J.Y., Min, N., Franzen, L., & Baker, H. (1996) Rapid down-regulation of tyrosine hydroxylase
870 expression in the olfactory bulb of naris-occluded adult rats. *J. Comp. Neurol.*, **369**, 264–276.
871 Cigola, E., Volpe, B.T., Lee, J.W., Franzen, L., & Baker, H. (1998) Tyrosine hydroxylase expression in
872 primary cultures of olfactory bulb: role of L-type calcium channels. *J. Neurosci.*, **18**, 7638–
873 7649.
874 Cockerham, R., Liu, S., Cachope, R., Kiyokage, E., Cheer, J.F., Shipley, M.T., & Puche, A.C. (2016)
875 Subsecond Regulation of Synaptically Released Dopamine by COMT in the Olfactory Bulb. *J.*
876 *Neurosci.*, **36**, 7779–7785.
877 Coppola, D.M. (2012) Studies of olfactory system neural plasticity: the contribution of the unilateral
878 naris occlusion technique. *Neural Plast.*, **2012**, 351752.
879 Cummings, D.M., Henning, H.E., & Brunjes, P.C. (1997) Olfactory bulb recovery after early sensory
880 deprivation. *J. Neurosci.*, **17**, 7433–7440.
881 Ennis, M., Zhou, F.M., Ciombor, K.J., Aroniadou-Anderjaska, V., Hayar, A., Borrelli, E., Zimmer, L.A.,
882 Margolis, F., & Shipley, M.T. (2001) Dopamine D2 receptor-mediated presynaptic inhibition
883 of olfactory nerve terminals. *J. Neurophysiol.*, **86**, 2986–2997.
884 Fogli Iseppe, A., Pignatelli, A., & Belluzzi, O. (2016) Calretinin-Periglomerular Interneurons in Mice
885 Olfactory Bulb: Cells of Few Words. *Front Cell Neurosci*, **10**, 231.
886 Fokkens, W.J., Lund, V.J., Mullol, J., Bachert, C., Alobid, I., Baroody, F., Cohen, N., Cervin, A., Douglas,
887 R., Gevaert, P., Georgalas, C., Goossens, H., Harvey, R., Hellings, P., Hopkins, C., Jones, N.,
888 Joos, G., Kalogjera, L., Kern, B., Kowalski, M., Price, D., Riechelmann, H., Schlosser, R., Senior,
889 B., Thomas, M., Toskala, E., Voegels, R., Wang, D.Y., & Wormald, P.J. (2012) EPOS 2012:
890 European position paper on rhinosinusitis and nasal polyps 2012. A summary for
891 otorhinolaryngologists. *Rhinology*, **50**, 1–12.
892 Galliano, E., Franzoni, E., Breton, M., Chand, A.N., Byrne, D.J., Murthy, V.N., & Grubb, M.S. (2018)
893 Embryonic and postnatal neurogenesis produce functionally distinct subclasses of
894 dopaminergic neuron. *Elife*, **7:**e32373.
895 Galliano, E., Hahn, C., Browne, L., Villamayor, P.R., & Grubb, M.S. (2021) Brief sensory deprivation
896 triggers cell type-specific structural and functional plasticity in olfactory bulb neurons. *J*
897 *Neurosci,* **41**, 2135-2151.
898 Grier, B.D., Belluscio, L., & Cheetham, C.E.J. (2016) Olfactory Sensory Activity Modulates Microglial-
899 Neuronal Interactions during Dopaminergic Cell Loss in the Olfactory Bulb. *Front Cell*
900 *Neurosci*, **10**, 178.
901 Hadjiconstantinou, M., Wemlinger, T.A., Sylvia, C.P., Hubble, J.P., & Neff, N.H. (1993) Aromatic L-
902 amino acid decarboxylase activity of mouse striatum is modulated via dopamine receptors. *J.*
903 *Neurochem.*, **60**, 2175–2180.
904 Halász, N., Ljungdahl, A., Hökfelt, T., Johansson, O., Goldstein, M., Park, D., & Biberfeld, P. (1977)
905 Transmitter histochemistry of the rat olfactory bulb. I. Immunohistochemical localization of
906 monoamine synthesizing enzymes. Support for intrabulbar, periglomerular dopamine
907 neurons. *Brain Res.*, **126**, 455–474.

908 Hayar, A., Karnup, S., Shipley, M.T., & Ennis, M. (2004) Olfactory Bulb Glomeruli: External Tufted
909 Cells Intrinsically Burst at Theta Frequency and Are Entrained by Patterned Olfactory Input. *J.*
910 *Neurosci.*, **24**, 1190–1199.
911 Heffner, C.S., Herbert Pratt, C., Babiuk, R.P., Sharma, Y., Rockwood, S.F., Donahue, L.R., Eppig, J.T., &
912 Murray, S.A. (2012) Supporting conditional mouse mutagenesis with a comprehensive cre
913 characterization resource. *Nat Commun*, **3**, 1218.
914 Hökfelt, T., Halasz, N., Ljungdahl, A., Johansson, O., Goldstein, M., & Park, D. (1975) Histochemical
915 support for a dopaminergic mechanism in the dendrites of certain periglomerular cells in the
916 rat olfactory bulb. *Neurosci. Lett.*, **1**, 85–90.
917 Hsia, A.Y., Vincent, J.D., & Lledo, P.M. (1999) Dopamine depresses synaptic inputs into the olfactory
918 bulb. *J. Neurophysiol.*, **82**, 1082–1085.
919 Kass, M.D., Pottackal, J., Turkel, D.J., & McGann, J.P. (2013) Changes in the neural representation of
920 odorants after olfactory deprivation in the adult mouse olfactory bulb. *Chem. Senses*, **38**,
921 77–89.
922 Kikuta, S., Sakamoto, T., Nagayama, S., Kanaya, K., Kinoshita, M., Kondo, K., Tsunoda, K., Mori, K., &
923 Yamasoba, T. (2015) Sensory deprivation disrupts homeostatic regeneration of newly
924 generated olfactory sensory neurons after injury in adult mice. *J. Neurosci.*, **35**, 2657–2673.
925 Kiyokage, E., Pan, Y.-Z., Shao, Z., Kobayashi, K., Szabo, G., Yanagawa, Y., Obata, K., Okano, H., Toida,
926 K., Puche, A.C., & Shipley, M.T. (2010) Molecular identity of periglomerular and short axon
927 cells. *J. Neurosci.*, **30**, 1185–1196.
928 Kohwi, M., Petryniak, M.A., Long, J.E., Ekker, M., Obata, K., Yanagawa, Y., Rubenstein, J.L.R., &
929 Alvarez-Buylla, A. (2007) A subpopulation of olfactory bulb GABAergic interneurons is
930 derived from Emx1- and Dlx5/6-expressing progenitors. *J. Neurosci.*, **27**, 6878–6891.
931 Kosaka, K. & Kosaka, T. (2007) Chemical properties of type 1 and type 2 periglomerular cells in the
932 mouse olfactory bulb are different from those in the rat olfactory bulb. *Brain Res.*, **1167**, 42–
933 55.
934 Kosaka, T. & Kosaka, K. (2011) “Interneurons” in the olfactory bulb revisited. *Neurosci. Res.*, **69**, 93–
935 99.
936 Kosaka, T., Kosaka, K., Hama, K., Wu, J.Y., & Nagatsu, I. (1987) Differential effect of functional
937 olfactory deprivation on the GABAergic and catecholaminergic traits in the rat main olfactory
938 bulb. *Brain Res.*, **413**, 197–203.
939 Kosaka, T., Pignatelli, A., & Kosaka, K. (2019) Heterogeneity of tyrosine hydroxylase expressing
940 neurons in the main olfactory bulb of the mouse. *Neurosci. Res.*,.
941 Lammel, S., Steinberg, E.E., Földy, C., Wall, N.R., Beier, K., Luo, L., & Malenka, R.C. (2015) Diversity of
942 transgenic mouse models for selective targeting of midbrain dopamine neurons. *Neuron*, **85**,
943 429–438.
944 Lau, C.G. & Murthy, V.N. (2012) Activity-dependent regulation of inhibition via GAD67. *J. Neurosci.*,
945 **32**, 8521–8531.
946 Liu, N., Cigola, E., Tinti, C., Jin, B.K., Conti, B., Volpe, B.T., & Baker, H. (1999) Unique regulation of
947 immediate early gene and tyrosine hydroxylase expression in the odor-deprived mouse
948 olfactory bulb. *J. Biol. Chem.*, **274**, 3042–3047.
949 Liu, S., Plachez, C., Shao, Z., Puche, A., & Shipley, M.T. (2013) Olfactory bulb short axon cell release of
950 GABA and dopamine produces a temporally biphasic inhibition-excitation response in
951 external tufted cells. *J. Neurosci.*, **33**, 2916–2926.
952 Liu, S., Puche, A.C., & Shipley, M.T. (2016) The Interglomerular Circuit Potently Inhibits Olfactory
953 Bulb Output Neurons by Both Direct and Indirect Pathways. *J. Neurosci.*, **36**, 9604–9617.
954 Livak, K.J. & Schmittgen, T.D. (2001) Analysis of Relative Gene Expression Data Using Real-Time
955 Quantitative PCR and the 2−ΔΔCT Method. *Methods*, **25**, 402–408.
956 Maher, B.J. & Westbrook, G.L. (2008) Co-transmission of dopamine and GABA in periglomerular
957 cells. *J. Neurophysiol.*, **99**, 1559–1564.

958 Mandairon, N., Sacquet, J., Jourdan, F., & Didier, A. (2006) Long-term fate and distribution of
959 newborn cells in the adult mouse olfactory bulb: Influences of olfactory deprivation.
960 *Neuroscience*, **141**, 443–451.
961 McGann, J.P. (2013) Presynaptic inhibition of olfactory sensory neurons: new mechanisms and
962 potential functions. *Chem. Senses*, **38**, 459–474.
963 Nadi, N.S., Head, R., Grillo, M., Hempstead, J., Grannot-Reisfeld, N., & Margolis, F.L. (1981) Chemical
964 deafferentation of the olfactory bulb: plasticity of the levels of tyrosine hydroxylase,
965 dopamine and norepinephrine. *Brain Res.*, **213**, 365–377.
966 Ninkovic, J., Pinto, L., Petricca, S., Lepier, A., Sun, J., Rieger, M.A., Schroeder, T., Cvekl, A., Favor, J., &
967 Götz, M. (2010) The transcription factor Pax6 regulates survival of dopaminergic olfactory
968 bulb neurons via crystallin αA. *Neuron*, **68**, 682–694.
969 Panzanelli, P., Fritschy, J.M., Yanagawa, Y., Obata, K., & Sassoè-Pognetto, M. (2007) GABAergic
970 phenotype of periglomerular cells in the rodent olfactory bulb. *Journal of Comparative*
971 *Neurology*, **502**, 990–1002.
972 Parrish-Aungst, S., Kiyokage, E., Szabo, G., Yanagawa, Y., Shipley, M.T., & Puche, A.C. (2011) Sensory
973 experience selectively regulates transmitter synthesis enzymes in interglomerular circuits.
974 *Brain Res.*, **1382**, 70–76.
975 Parrish-Aungst, S., Shipley, M.T., Erdelyi, F., Szabo, G., & Puche, A.C. (2007) Quantitative analysis of
976 neuronal diversity in the mouse olfactory bulb. *J. Comp. Neurol.*, **501**, 825–836.
977 Philpot, B.D., Men, D., McCarty, R., & Brunjes, P.C. (1998) Activity-dependent regulation of
978 dopamine content in the olfactory bulbs of naris-occluded rats. *Neuroscience*, **85**, 969–977.
979 Pignatelli, A., Ackman, J.B., Vigetti, D., Beltrami, A.P., Zucchini, S., & Belluzzi, O. (2009) A potential
980 reservoir of immature dopaminergic replacement neurons in the adult mammalian olfactory
981 bulb. *Pflugers Arch.*, **457**, 899–915.
982 Pignatelli, A. & Belluzzi, O. (2017) Dopaminergic Neurones in the Main Olfactory Bulb: An Overview
983 from an Electrophysiological Perspective. *Front Neuroanat*, **11**, 7.
984 Pignatelli, A., Kobayashi, K., Okano, H., & Belluzzi, O. (2005) Functional properties of dopaminergic
985 neurones in the mouse olfactory bulb. *J. Physiol. (Lond.)*, **564**, 501–514.
986 Pinching, A.J. & Powell, T.P. (1971) The neuropil of the periglomerular region of the olfactory bulb. *J.*
987 *Cell. Sci.*, **9**, 379–409.
988 Rosser, A.E., Hökfelt, T., & Goldstein, M. (1986) LHRH and catecholamine neuronal systems in the
989 olfactory bulb of the mouse. *Journal of Comparative Neurology*, **250**, 352–363.
990 Saino-Saito, S., Sasaki, H., Volpe, B.T., Kobayashi, K., Berlin, R., & Baker, H. (2004) Differentiation of
991 the dopaminergic phenotype in the olfactory system of neonatal and adult mice. *J. Comp.*
992 *Neurol.*, **479**, 389–398.
993 Sato, T., Homma, R., & Nagayama, S. (2020) Direct comparison of odor responses of homologous
994 glomeruli in the medial and lateral maps of the mouse olfactory bulb. *eNeuro*,.
995 Short, S.M. & Wachowiak, M. (2019) Temporal Dynamics of Inhalation-Linked Activity across Defined
996 Subpopulations of Mouse Olfactory Bulb Neurons Imaged In Vivo. *eNeuro*, **6**.
997 Stone, D.M., Grillo, M., Margolis, F.L., Joh, T.H., & Baker, H. (1991) Differential effect of functional
998 olfactory bulb deafferentation on tyrosine hydroxylase and glutamic acid decarboxylase
999 messenger RNA levels in rodent juxtaglomerular neurons. *J. Comp. Neurol.*, **311**, 223–233.
1000 Stone, D.M., Wessel, T., Joh, T.H., & Baker, H. (1990) Decrease in tyrosine hydroxylase, but not
1001 aromatic L-amino acid decarboxylase, messenger RNA in rat olfactory bulb following
1002 neonatal, unilateral odor deprivation. *Brain Res. Mol. Brain Res.*, **8**, 291–300.
1003 Tavakoli, A., Schmaltz, A., Schwarz, D., Margrie, T.W., Schaefer, A.T., & Kollo, M. (2018) Quantitative
1004 Association of Anatomical and Functional Classes of Olfactory Bulb Neurons. *J. Neurosci.*, **38**,
1005 7204–7220.
1006 Taylor, S.C., Nadeau, K., Abbasi, M., Lachance, C., Nguyen, M., & Fenrich, J. (2019) The Ultimate qPCR
1007 Experiment: Producing Publication Quality, Reproducible Data the First Time. *Trends in*
1008 *Biotechnology*, **37**, 761–774.

1009 Vaaga, C.E., Yorgason, J.T., Williams, J.T., & Westbrook, G.L. (2017) Presynaptic gain control by
1010 endogenous cotransmission of dopamine and GABA in the olfactory bulb. *J. Neurophysiol.*,
1011 **117**, 1163–1170.
1012 Vlug, A.S., Teuling, E., Haasdijk, E.D., French, P., Hoogenraad, C.C., & Jaarsma, D. (2005) ATF3
1013 expression precedes death of spinal motoneurons in amyotrophic lateral sclerosis-SOD1
1014 transgenic mice and correlates with c-Jun phosphorylation, CHOP expression, somato-
1015 dendritic ubiquitination and Golgi fragmentation. *Eur. J. Neurosci.*, **22**, 1881–1894.
1016 Wachowiak, M., Economo, M.N., Díaz-Quesada, M., Brunert, D., Wesson, D.W., White, J.A., &
1017 Rothermel, M. (2013) Optical dissection of odor information processing in vivo using
1018 GCaMPs expressed in specified cell types of the olfactory bulb. *J. Neurosci.*, **33**, 5285–5300.
1019 Wang, M., Cai, E., Fujiwara, N., Fones, L., Brown, E., Yanagawa, Y., & Cave, J.W. (2017) Odorant
1020 Sensory Input Modulates DNA Secondary Structure Formation and Heterogeneous
1021 Ribonucleoprotein Recruitment on the Tyrosine Hydroxylase and Glutamic Acid
1022 Decarboxylase 1 Promoters in the Olfactory Bulb. *J. Neurosci.*, **37**, 4778–4789.
1023 Weiss, J., Pyrski, M., Jacobi, E., Bufe, B., Willnecker, V., Schick, B., Zizzari, P., Gossage, S.J., Greer,
1024 C.A., Leinders-Zufall, T., Woods, C.G., Wood, J.N., & Zufall, F. (2011) Loss-of-function
1025 mutations in sodium channel Nav1.7 cause anosmia. *Nature*, **472**, 186–190.
1026 Wilson, D.A. & Sullivan, R.M. (1995) The D2 antagonist spiperone mimics the effects of olfactory
1027 deprivation on mitral/tufted cell odor response patterns. *J. Neurosci.*, **15**, 5574–5581.
1028 Zeisel, A., Hochgerner, H., Lönnerberg, P., Johnsson, A., Memic, F., van der Zwan, J., Häring, M.,
1029 Braun, E., Borm, L.E., La Manno, G., Codeluppi, S., Furlan, A., Lee, K., Skene, N., Harris, K.D.,
1030 Hjerling-Leffler, J., Arenas, E., Ernfors, P., Marklund, U., & Linnarsson, S. (2018) Molecular
1031 Architecture of the Mouse Nervous System. *Cell*, **174**, 999-1014.e22.
1032 Zhu, M.Y., Juorio, A.V., Paterson, I.A., & Boulton, A.A. (1993) Regulation of striatal aromatic L-amino
1033 acid decarboxylase: effects of blockade or activation of dopamine receptors. *Eur. J.*
1034 *Pharmacol.*, **238**, 157–164.
1035